Clusters with close packing and filled shells

B. M. Smirnov

Institute of High Temperatures, Russian Academy of Sciences, Moscow

Sequences of clusters with a short-range interaction of atoms which form symmetrical structures are constructed. Expressions for cluster parameters of some sequences at zero temperature are obtained within the framework of a general scheme. Distributions of atoms on cluster shells at finite temperatures are evaluated. An analysis sets up a correspondence between parameters of large clusters and macroscopic particles or macroscopic surfaces. The nature of the solid-liquid phase transition for clusters and other systems of atoms with a short-range interaction is discussed.

1. INTRODUCTION

A short-range interaction of atoms in the attraction region is characterized by a narrow and shallow well in the interaction potential. Then only pair interaction between nearest neighbors takes place in a cluster—a system of bound atoms. Besides, the interaction potential of two nearest atoms does not depend on interaction of these atoms with others. This atomic system is well described by models in which atoms are replaced by balls. For hard ball models the distance between nearest neighbors is fixed, and the resultant structures are said to be structures with close packing. There are such structures in crystals with the cubic face-centered and hexagonal lattice.[1-4] Other structures, in which the distances between nearest neighbors vary within some interval, are modeled by soft balls. The main example of such a cluster structure is the icosahedron one.[5] This is the frequently occurring cluster structure which atoms form inside metals, alloys and other condensed systems. Because of its importance, we consider this structure together with the close packed ones.

A cluster with close packing has a high symmetry which is conserved in various geometric figures that cluster atoms can form—octahedra, dodecahedra etc. The analysis of symmetric structures of clusters[6-22] gives information concerning the energy parameters of such clusters. Recently a simple method for the analysis of clusters with cubic face-centered structure was developed.[23,24] It allows one to evaluate the energy parameters of clusters consisting of hundreds of atoms for various distributions of cluster atoms. The aim of this paper is to analyze various symmetric structures of clusters with a short-range interaction of atoms by using this method and the information contained in Refs. 6-22 for such clusters. This analysis admits generalizations which allow one to describe closed structures with soft packing, such as the icosahedral structures.

The close-packed structures under consideration due to their high symmetry are suitable models for the analysis of large clusters which have recently been the subject of detailed studies.[25-30] The main group of problems is the transition from clusters to macroscopic systems which occurs in different ways depending on cluster types and parameters under consideration. Results of the analysis of symmetrical cluster structures within the framework of the above question give additional information in understanding the character of the transition from molecules to macroscopic systems as the number of atoms in the systems is increased. Besides, the study of melting for clusters with close packing supplements our knowledge of physics of the phase transition with new details. It confirms us that melting of a condensed system of atoms with a short-range interaction is determined by transition between structures which are formed from neighboring atoms inside the system.

Note that the above questions are of interest not only as methodological ones. Because of a short-range interaction of inert gas atoms, the results relate to clusters and condensed inert gases.

2. SHORT-RANGE INTERACTION IN ATOMIC PHYSICS

The concept of a short-range interaction has arisen in nuclear physics for nucleon interaction. For example, the Yukawa interaction potential of two nucleons has the form:[31,32]

$$U(R) = U_0 e^{-\alpha R}. \tag{1}$$

Here R is the distance between nucleons, $1/\alpha = \hbar/(m_\pi c)$ is the range of nuclear forces, m_π is the π-meson mass, c is the light velocity. If a region of distances under consideration significantly exceeds the range of nuclear forces this potential can be written in the form:

$$U(r) = U_0 \delta(\mathbf{R})/\alpha. \tag{2}$$

It is the potential of a short-range interaction in nuclear physics. As it is seen its maximum corresponds to small distances between nucleons.

One can extend the concept of a short-range interaction also to the interaction of atoms or molecules by postulating the width of the region of distances between atoms where atomic interaction is important to be small. In contrast to the nuclear physics case, atomic interaction must include both attraction and repulsion. Besides the maximum attraction corresponds to finite distances between the atoms.

It is convenient to use the following approximate expression for the interaction potential of two atomic particles:

$$U(R) = \frac{D}{l-k} [k(R_e/R)^l - l(R_e/R)^k].$$ (3)

Here R is the distance between atomic particles, R_e is the equilibrium distance which corresponds to maximum attraction, D is the maximum depth of the potential well, k,l are parameters. The Lennard–Jones potential corresponds to the case $k=6$, $l=12$:

$$U(R) = D[(R_e/R)^{12} - 2(R_e/R)^6].$$ (4)

The short-range interaction potential relates to values of parameters of formula (3) $k,l \gg 1$.

Some gaseous processes are determined solely by the repulsive part of the interaction potential (for instance, transport coefficients), other effects are determined only by the attractive region of interaction. Therefore it is convenient to divide the interaction potential into two parts: the repulsive and attractive regions. Further we use only the attractive part of the interaction potential which is characterized by a narrow and shallow well, and is of interest for bound atomic systems. Because of the condition of the small depth of the potential well the interaction potential of two interacting atoms does not depend on their interaction with other nearest neighbors in a system of many bound atoms. Then the total interaction potential of such a system is the sum of pair interaction potentials of atoms—nearest neighbors.

The form of the interaction potential under consideration allows us to approximate atoms by balls. In the approximation of a narrow well for an attractive interaction or an infinite wall for a repulsive one these balls are hard. In particular, the corresponding model of the repulsive potential which is used for calculation of transport coefficients of gases is called the hard sphere model and is a basis for an analysis of transport phenomena in gases.[33-36] Accepting a finite width Δr of the attractive well, one can consider balls of the above models to be soft.

Further due to the model character of the analysis of clusters we neglect the long-range interaction of atoms. It means that the attractive potential is represented in the form (see Fig. 1):

$$U(R) = -D + U''(R_e) \cdot (R - R_e)^2, \quad R_1 < R < R_2,$$

$$= 0, \quad R < R_1, \quad R > R_2,$$ (5a)

where $R_1, R_2 = R_e \pm \sqrt{D/U''}$, $^{1/2} U''$ is the second derivative of the actual interaction potential at its minimum.

The following form of the interaction potential of atoms is more convenient for applications:

$$U(R) = D \exp[-(R - R_e)^2/2\Delta r^2],$$ (5b)

where $\Delta r = [D/U''(R_e)]^{1/2}$. To estimate the accuracy of such an approximation note that the value $\int U(R)dR$ for the Lennard–Jones potential (4) and the potential (5b) with the same value of $U''(R_e)$ differ by 20%.
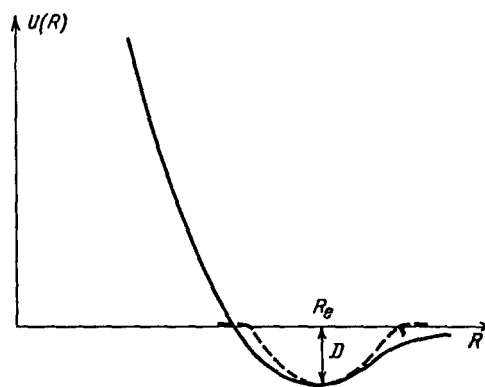

FIG. 1. The interaction potential of two atoms (solid line) and the attraction model potential for short-range interaction (dotted line).

Ball models for description of systems under consideration are valid for classical atoms. This condition corresponds to the condition of a narrow and shallow potential well if the atom mass is large and satisfies the criterion:

$$m \gg \hbar^2 U''/D^2.$$

It follows from the condition of a small vibrational energy of the diatomic molecule compared with its dissociation energy.

As we have noted above, the interaction of two atoms of inert gases is a short-range one, and the results given below relate to condensed inert gas systems. Therefore Table I lists the parameters of the pair interaction potential for inert gas atoms.[37-39] Note that systems of atoms with a short-range interaction are characterized by a certain scaling law. Indeed, the parameters of a system of bound atoms with a short range interaction are expressed through the following parameters: R_e—the equilibrium distance for the diatomic molecule constructed from interacting atoms, D—the depth of the interaction well, m—the atom mass.

TABLE I. Parameters of diatomic molecules of inert gases and reduced parameters of condensed inert gases.

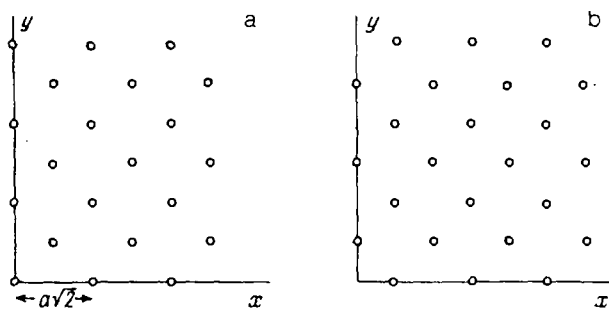| Parameter	Ne	Ar	Kr	Xe	Average
D, meV	3,7	12,2	17,2	24	—
R_e, Å	3,09	3,76	4,01	4,36	—
$\hbar\omega$, cm^{-1}	26	14	24	21	—
$\Delta r/R$	0,16	0,094	0,077	0,077	0,10 ± 0,04
a/R_e	1,02	1,00	1,00	0,99	1,00 ± 0,01
ε_{sub}/D	5,4	6,6	6,7	7,1	6,4 ± 0,7
T_m/D	0,57	0,59	0,58	0,58	0,58 ± 0,01
T_b/D	0,63	0,62	0,60	0,59	0,61 ± 0,02
ρ_s/ρ_0	0,90	0,92	0,93	0,95	0,93 ± 0,02
$1 - (\rho_l/\rho_s)$	0,137	0,126	0,136	0,131	0,132 ± 0,005
$1 - (\rho_b/\rho_s)$	0,165	0,151	0,146	0,156	0,154 ± 0,008
$\Delta H_{mel}/D$	0,94	1,00	0,99	0,99	0,98 ± 0,03
$\varepsilon_{ev}/6D$	0,82	0,92	0,91	0,91	0,89 ± 0,04

FIG. 2. Positions of centers of atoms on the symmetry plane for the cubic face-centered lattice (a) and at the distance $\pm a/\sqrt{2}$ from it (b). Further such layers are alternated. Due to symmetry the same distribution of atoms corresponds to planes xz and yz.

Table I contains parameters of condensed inert gases expressed in reduced units. The following notations are used: a—the distance between neighboring atoms of an inert gas at zero temperature; ρ_0—the crystal density at zero temperature; ρ_s—the crystal density at the melting point; ρ_f—the liquid density at the melting point; ρ_b—the liquid density at the boiling point; T_m, T_b—the melting and boiling points correspondingly; ε_{sub}—the sublimation energy of the crystal at zero temperature relating to one atom; ΔH_{mel}—the melting heat per atom; ε_{ev}—the energy which is spent for evaporation of one atom at the boiling point.

It follows from Table I that a short-range interaction describes condensed inert gas systems satisfactorily and is better than the Lennard–Jones interaction potential (In the case of the Lennard-Jones potential we have[1] $a = 0.99 R_e$, $\varepsilon_{sub} = 8.61 D$, while the short range interaction potential gives $a = R_e$, $\varepsilon_{sub} = 6 D$). Therefore it is valid to use the short range interaction for description of bound systems of inert gas atoms. The degree of coincidence for reduced parameters of different inert gases in Table I characterizes the accuracy of using the pair short-range interaction for description of condensed inert gases or their clusters.

3. ASSEMBLING OF CLUSTERS WITH CLOSE PACKING

Let us describe the method of construction of clusters with close packing[23] and analyze the energy parameters of such clusters. There are two types of crystals with close packing which have the cubic face-centered or hexagonal lattice.[1-4] In both cases each atom of the structure has 12 nearest neighbors, but the symmetry of these structures is different. Below we shall be guided by the cubic face-centered structure. Take one atom of such a lattice as an origin and choose a frame of axes zxy corresponding to Fig. 2. In this frame of axes the nearest neighbors of the central atom have the coordinates 0, $\pm a/\sqrt{2}$, $\pm a/\sqrt{2}$; $\pm a/\sqrt{2}$, 0, $\pm a/\sqrt{2}$; $\pm a/\sqrt{2}$, $\pm a/\sqrt{2}$, 0, where a is the distance between nearest neighbors.

As may be seen, in the frame of axes under consider-ation the infinite cubic face-centered lattice is preserved under two types of transformation:

1) $x \rightleftarrows y \rightleftarrows z$,

2) $x \rightleftarrows -x$; $y \rightleftarrows -y$; $z \rightleftarrows -z$. (6)

One can use such a symmetry of clusters as the basis for assembling clusters with close packing. Then this operation of cluster construction is equivalent to cutting out the cluster from the crystal with the cubic face-centered structure.

It is convenient to introduce reduced values for atomic coordinates expressing them in units of $a/\sqrt{2}$. Then the z, x, y coordinates of each atom are integers and their sum is an even integer. Because of the cluster symmetry the operation of assembling a cluster corresponds to placing atoms on cluster shells, and coordinates of all atoms of one shell can be obtained from the coordinates of one atom as a result of transformations (6). This allows us to use for cluster description the coordinates of one atom from each shell. Further we choose atoms with positive values of coordinates and $z \leqslant x \leqslant y$.

On the basis of this let us calculate the number of nearest neighbors for atoms of a given shell. Because the cluster energy is determined by the number of bonds in the cluster, it allows us to calculate the cluster energy, the cohesive energy of atoms attached to the cluster and to find the optimal sequence of occupation of shells at zero temperature. Let us analyze the corresponding results.

Since the distance between neighboring atoms is fixed, the binding energy for two nearest neighbors is equal to D. Therefore the total binding energy of atoms in a cluster is:

$$E = kD, \qquad (7)$$

where k is the total number of bonds between nearest neighbors. Further we express the energy in units of D, i.e. the binding energy of cluster atoms is equal to the total number of bonds between nearest neighbors.

For large numbers of cluster atoms n most of the atoms are located inside the cluster and have 12 nearest neighbors. Therefore there is the asymptotic dependence $E(n) \rightarrow 6n$ for $n \rightarrow \infty$. It is convenient to introduce the surface energy E_{sur} as:

$$E_{sur} = 6n - E. \qquad (8)$$

Another expression for the surface energy has the form:

$$E_{sur} = \sum_k \left(6 - \frac{k}{2} \right) n_k, \qquad (9)$$

where n_k is the number of atoms that have k nearest neighbors. From this it follows that addition of an atom with k nearest neighbors to the cluster increases the cluster surface energy by the amount $6 - k$. We used the fact that one bond relates to two atoms.

Constructing the cluster under consideration at zero temperature, we postulate that its optimal structure corresponds to a minimum surface energy for a given number of cluster atoms. This characterizes the sequence of the growth of the cluster as a result of addition of new atoms to it. This sequence of cluster growth is given in Table II

TABLE II. Sequence of the growth of clusters with close packing.

Shells being filled *)	n	E_{sur}	$v \cdot w$
011 (1–5)	2–13	6–42	12 · 1
002 (4)	13–19	42–54	6 · 1
112 (3–5) + 022 (5)	19–55	54–114	12 · 3
013 (4–6)	55–79	114–138	6 · 4
123 (3–5) + 222 (6)	79–135	138–210	8 · 7
033 (5)	135–147	210–222	12 · 1
004 (4) + 114 (5) + 024 (6)	147–201	222–258	6 · 9
233 (3–5) + 224 (5) + 134 (5–6)	201–297	258–354	8 · 12
015 (4–6) + 125 (5–6)	297–369	354–402	6 · 12
044 (5) + 035 (6)	369–405	402–414	12 · 3
006 (4) + 116 (5) + 026 (6)	405–459	414–450	6 · 9
334 (3–5) + 244 (5) + 235 (5–6) + 145 (5–6) + 226 (5) + 136 (6)	459–675	450–594	8 · 27
055 (5) + 046 (6)	675–711	594–606	12 · 3
017 (4–6) + 127 (5–6) + 037 (6)	711–807	606–654	6 · 16
008 (4) + 118 (5) + 028 (6)	807–861	654–690	6 · 9
444 (4–6) + 345 (4–6) + 255 (5) + 336 (5) + 246 (6) + 156 (5–6) + + 237 (5—6) + 147 (6)	861–1157	690–858	8 · 37
066 (5) + 057 (6) + 228 (5) + 138 (6) + 048 (6)	1157–1289	858–894	12 · 11
019 (4–6) + 129 (5–6) + 039 (6)	1289–1385	894–942	6 · 16
455 (3–5) + 446 (5) + 356 (5–6) + 347 (5–6) + 266 (5) + 257 (6) + + 338 (5) + 248 (6) + 158 (6) + 167 (5—6) + 239 (5–6) + 149 (6)	1385–1865	942–1158	8 · 60
077 (5) + 068 (6) + 059 (6)	1865–1925	1158–1170	12 · 5
00,10 (4) + 11,10 (5) + 12,10 (6) + 22,10 (5) + 13,10 (6) + 04,10 (6)	1925–2075	1170–1230	6 · 25
01,11 (4–6) + 12,11 (5–6) + 03,11 (6)	2075–2171	1230–1278	6 · 16

*)Values in parentheses show the number of nearest neighbors.

which is an expanded version of the analysis of Refs. 23 and 24. It is seen that small clusters can grow as a result of the occupation of separate shells, but for large clusters the simultaneous filling of several shells takes place. Thus cluster growth results from the addition of separate blocks to the cluster with close packing. In Table II v is the number of separate blocks which have no common boundaries, and w is the number of atoms in a filled block. The shell and block structure of clusters is observed for metallic[37–41] and other types[42–44] of large clusters.

Note that the sequence of cluster growth of Table II has a schematic character for some cases of large clusters. For example, a cluster with about 500 atoms grows by addition of blocks with 27 atoms in each. But after addition of three such blocks attachment of atoms from shells 055 and 066 is favored. For large clusters such violation of the sequence of cluster growth occurs more often. Because it is not essential at finite temperatures we will not dwell on this in detail.

4. THE CUBO-OCTAHEDRAL CLUSTER STRUCTURE

Clusters with closed shells are not changed as a result of the transformations (6). This property is fulfilled for some symmetric figures which can form clusters with close packing. Using the experience of the analysis of such clusters (Refs. 6–22), we study some of these further within the framework of a general scheme using their symmetry (6). It leads to analytical expressions for energy parameters of these clusters and allows us to analyze them as systems of many bound atoms. Further we consider such figures as cubo-octahedron, cube, octahedron and tetra-

kaidecahedron. Such an analysis is of interest because it is carried out within the framework of a general scheme that unites various structures and allows one to pick out the optimal ones. Besides, it allows one to analyze general properties of these structures.

Figure 3 contains the simplest cubo-octahedral cluster consisting of 13 atoms which are modeled by hard balls, and Fig. 4 (Ref. 20) represents the cubo-octahedral cluster consisting of 55 atoms. The cubo-octahedral figure has a surface consisting of 6 squares and 8 triangles. It contains 24 common sides and 12 vertices. The distance between nearest neighbors for the cubo-octahedral structure is fixed. Therefore assuming vertices to be centers of the remotest atoms, we have the sides length for the figure surface is equal to ma, where a is the distance between nearest neighbors, m is the number of the surface layer.

Cubo-octahedrons have two modifications (see Fig. 3). In the first of these the projections of upper and lower triangles onto a plane parallel to them are the same (the hexagonal structure), in the second one these projections are turned by an angle $\pi/3$ around the axis which is perpendicular to the planes of triangles and passes through their centers (the cubic face-centered structure). This axis is the symmetry one for a cubo-octahedron. The figure is preserved as a result of turning around this axis by the angle $2\pi/3$. There are 4 such axes which pass through centers of opposite triangles. One more type of symmetry corresponds to reflection of the figure with respect to planes which pass through its center. For the first modification (the hexagonal structure) a cubo-octahedron is preserved as a result of reflection with respect to symmetry
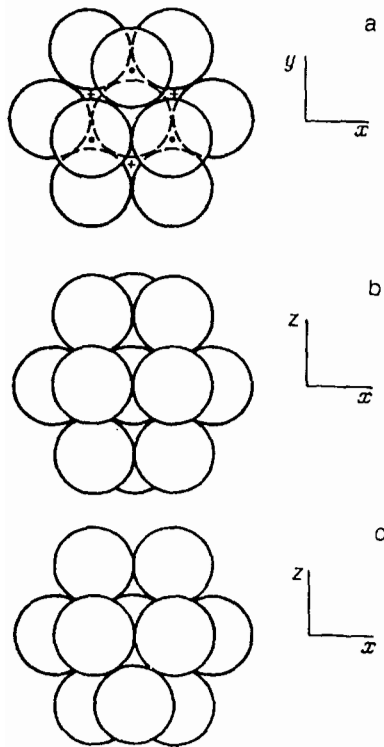
FIG. 3. Cubo-octahedron cluster consisting of 13 atoms. a) Positions of 3 atoms of the upper layer and 7 atoms of the central layer are given. Positions of centers of atoms of the lower layer are marked by crosses for the hexagonal structure and by circles for the cubic face-centered one. b,c) The front view for the hexagonal and cubic face-centered structure respectively.

planes (i.e. if the axis of a cubo-octahedron is Oz, it means $x \leftrightarrows -x$; $z \leftrightarrows -z$). For the cubic face-centered structure case a cubo-octahedron is preserved as a result of reflection $x \leftrightarrows -x$ and inversion $z \rightleftarrows -z$, $y \rightleftarrows -y$ (see Fig. 3).

As can be seen, a cubo-octahedron has a high symmetry and is one of the structures with close packing. Therefore it can be included in a general scheme of construction of clusters with close packing (see Table II). In the utilized notations the cluster-cubo-octahedron with mth closed shell includes atomic shells α, β, γ, where $\alpha, \beta, \gamma \leqslant m$ and $\alpha + \beta + \gamma \leqslant 2m$.
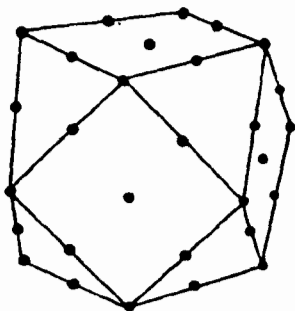

FIG. 4. Cubo-octahedron cluster consisting of 55 atoms and positions of centers of surface atoms.[20]

Let us evaluate the number of atoms in the surface layer of a cluster-cubo-octahedron. Denote the number of vertices by $p = 12$, the number of faces by $q = 24$, the number of squares by $r = 6$ and the number of triangles by $s = 8$. We have for the number of atoms on the surface of a closed layer:

$$\Delta n = p + q(m-1) + r(m-1)^2 + s(m-1)(m-2)/2$$
$$= 10m^2 + 2. \tag{10}$$

From this it follows that the expression for the total number of atoms of the cluster-cubo-octahedron:

$$n = 10m^3/3 + 5m^2 + 11m/3 + 1. \tag{11}$$

The cubo-octahedral structure allows us to analyze the connection between structures with close packing. For this purpose let us transfer from the frame of axes of Fig. 3 to the frame of axes of Fig. 2 where a cluster with the cubic face-centered structure has the symmetry with respect to the transformations (6). One can make such a transfer as a result of two turns around the x and z axes. Let us make a turn around the x axis through an angle φ. An atom with the coordinates zxy has the following coordinates $z'xy'$ in a new frame of axes:

$$z' = z \cos \varphi + y \sin \varphi,$$

$$y' = -z \sin \varphi + y \cos \varphi,$$

where $\cos \varphi = 1/\sqrt{3}$, $\sin \varphi = \sqrt{2/3}$. A subsequent rotation around the Oz axis through an angle $\pi/4$ corresponds to the following transformation for the new coordinates ZXY:

$$X = x/\sqrt{2} + y'/\sqrt{2},$$

$$Y = x/\sqrt{2} - y'/\sqrt{2}.$$

As a result of the above transformations we transfer from the frame of axes zxy of Fig. 3 to the frame of axes ZXY of Fig. 2. There are 48 different ways for transition from the frame of axes of Fig. 3 to the frame of axes of Fig. 2. Coordinates of atoms in the new frame of axes obtained as the result of different ways are connected by the transformations (6).

We now determine the positions of atoms of a cluster-cubo-octahedron for a new frame of axes. We choose, as before, as the unit of length $a/\sqrt{2}$, where a is the distance between the center and the vertices of the cubo-octahedron. In these units we have the following coordinates of vertices for the cluster-cubo-octahedron with the cubic face-centered structure in the new frame of axes:

$$0, \ \pm 1, \ \pm 1; \quad \pm 1, \ 0, \ \pm 1; \quad \pm 1, \ \pm 1, \ 0.$$

9 atoms of the cubo-octahedron with the hexagonal structure have the same positions as in the case of the cubic face-centered one, 3 atoms of the upper triangles of Fig. 3a occupy other positions. Instead of coordinates

$$0, \ 1, \ -1; \quad 1, \ 1, \ 0; \quad 1, \ 0, \ -1;$$

they have coordinates

$$4/3, \ 1/3, \ 1/3; \quad 1/3, \ 4/3, \ -1/3; \quad 1/3, \ 1/3, \ -4/3.$$

TABLE III. Parameters of the cubo-octahedron cluster.

m	n	E_{sur}	E_{opt}
1	13	42	42
2	55	114	114
3	147	222	220
4	309	366	362
5	561	546	535
6	923	762	729
7	1415	1014	963
8	2057	1302	1226

TABLE IV. Parameters of the cube cluster.

m	n	E_{sur}	E_{opt}
1	63	138	118
2	365	468	399
3	1099	978	828
4	2457	1686	1387 ± 11

As can be seen the symmetry of the cluster-cubo-octahedron with the hexagonal structure is mainly hidden in the frame of axes of Fig. 2. Indeed, the simple transformations which preserve the structure have the form $Z \rightleftarrows Y$, $X \rightleftarrows -Z$, $Y \rightleftarrows X$, and $Z \rightleftarrows -X$, $X \rightleftarrows Y$, $Y \rightleftarrows -Z$. Thus, the new frame of axes is not suitable for the analysis of clusters with the hexagonal structure because it exposes only part of the cluster symmetry. On the contrary, in this frame of axes clusters with the cubic face-centered structure have a high symmetry which is characterized by the transformations (6). Therefore the further analysis of clusters with close packing refers only to clusters with the cubic face-centered structure although we shall often refer to it as the structure with close packing.

Note that both the cubo-octahedral structure and other symmetrical structures under consideration have been studied previously Refs. 16–21, and the accumulated experience in this regard is used below. But usually the analysis is based on the Lennard–Jones interaction potential, which includes a long-range part of the interaction. Our task is simpler because of the absence of a long-range interaction. It allows us to obtain analytic expressions for energy parameters of clusters, while the presence of a long-range interaction demands numerical calculations. In addition remember that a short-range interaction describes inert gas crystals better than the Lennard–Jones interaction potential.

Let us determine the energy of the cluster with the cubo-octahedral structure. Take into account that each internal atom has 12 nearest neighbors and surface atoms have the following numbers of nearest neighbors: vertex atoms—5, edge atoms—7, atoms on squares—8, atoms on triangles—9. Using the number of atoms on each structure element, we obtain for the surface energy of the cluster-cubo-octahedron with m-closed layers (in units D):

$$E_{sur} = 18m^2 + 18m + 6. \qquad (12)$$

The total binding energy of atoms in the cluster-cubo-octahedron is equal to:

$$E = 6n - E_{sur} = 20m^3 + 12m^2 + 4m. \qquad (13)$$

Table III lists the surface energies of cubo-octahedron-clusters (E_{sur}) with closed layers which are compared with the surface energies E_{opt} of clusters with close packing and optimal configuration of atoms for a given n and at zero temperature. As may be seen, the cubo-octahedral structure is not the optimal one for clusters with close packing.

Indeed, assembling of a cluster-cubo-octahedron is finished with occupation of its vertices which have positions $0,m,m$ (notations of Table II). Table II shows that only the cubo-octahedral structures with $m=1$ and $m=2$ are optimal ones. For large m the cubo-octahedral structure is not optimal.

5. SYMMETRICAL STRUCTURES OF CLUSTERS WITH CLOSE PACKING

Now we study some structures with close packing within the framework of the scheme under consideration. These structures have the form of regular geometrical figures with plane surfaces and have been investigated previously Refs. 15–22 by numerical methods. From the standpoint of the method under consideration we have a certain sequence of closed shells. At first we analyze within the framework of the scheme under consideration the simplest structure—a cube. Its surface is a square net, its vertices relate to the shell $2m$, $2m$, $2m$; where m is the number of the figure in the sequence. Atoms at the cube edges have positions α, $2m$, $2m$, where $\alpha < 2m$ and is an even number. Surface atoms inside squares correspond to shells α, β, $2m$, where α, $\beta < 2m$. Note that atomic layers of this figure which are adjacent to surface layers do not have a square net. Projections of their atoms onto a neighboring surface layer are located in centers of squares which are formed by surface atoms. These two types of layers are alternated in a cluster-cube, i.e. the cluster has a complicated structure.

The cluster under consideration has $p=8$ vertices, $q=12$ edges and $r=6$ squares. Thus a surface layer contains p vertex atoms, $q(2m-1)$ edge atoms and $r(8m^2-4m+1)$ atoms inside squares. Each vertex atom has 3 nearest neighbors, each edge atom has 5 nearest neighbors and each atom inside a square has 8 nearest neighbors.

This gives for the number of atoms of a cube-cluster n and its surface energy E_{sur}:

$$n = 32m^3 + 24m^2 + 6m + 1,$$
$$E_{sur} = 96m^2 + 36m + 6. \qquad (14)$$

Comparison of the surface energies for the cube-clusters with closed layers and clusters with close packing of the optimal structure with the same number of atoms is provided in Table IV. Evidently, the cube-structure is far from the optimal structure of clusters with close packing.

Figure 5 gives the following cluster structure—the octahedral one. Its surface consists of 8 regular triangles. Atoms of this cluster occupy shells α, β, γ, where $\alpha + \beta + \gamma \leqslant 2m$ and m is an integer which characterizes the num-

FIG. 5. Octahedron cluster consisting of 231 atoms and positions of centers of surface atoms.

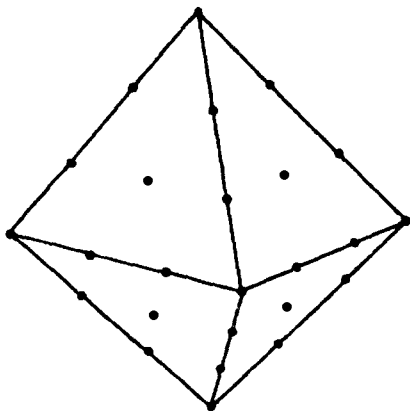FIG. 6. Tetrakaidecahedron cluster consisting of 201 atoms and positions of centers of surface atoms.[20]

ber of a figure in the sequence. The octahedral surface has $p=6$ vertices, $q=12$ edges and includes $s=8$ triangles. There are $q(2m-1)$ atoms in octahedron edges and $s(2m^2-3m+1)$ atoms inside triangles. Vertex atoms relate to a shell 0, 0, $2m$, atoms inside edges occupy shells 0, 1, $2m-1$, where 1 is an integer; atoms inside triangles form shells α, β, γ, where $\alpha+\beta+\gamma=2m$, α, β, $\gamma \geqslant 0$. Each vertex atom has 4 nearest neighbors, each edge atom has 7 nearest neighbors, and each atom inside triangles has 9 nearest neighbors. From this we obtain the following expressions for the total number of atoms n for a cluster-octahedron and its surface energy E_{sur}:

$$n=16m^3/3+8m^2+14m/3+1,$$
$$E_{sur}=24m^2+24m+6. \qquad (15)$$

Table V lists parameters of octahedron-clusters that follow from these formulae and the surface energies for optimal configurations of clusters with close packing E_{opt} and a given n.

The analysis of the above data for various cluster structures shows that the number of nearest neighbors for vertex atoms is less than for other surface atoms. One can expect that the figure will be close to the optimal one if the vertex atoms are cut off. Indeed, such a truncated structure is closer to the spherical one than the original one. Consider one of such structures—tetrakaidecahedron[20] (Fig. 6) which is formed from an octahedron as a result of cutting off its vertex pyramids. The surface of a tetrakaidecahedron consists of 8 regular hexagons and 6 squares. Note

that a tetrakaidecahedron can be obtained only from octahedra for which m is a number divisible by three.

Introducing a tetrakaidecahedron number m, we have that it contains $p=24$ vertices which occupy a shell $0,2m,4m$, $q'=12$ edges which are common sides of hexagons and belong to shells $0,\beta,\gamma$, where $\beta+\gamma=6m$, $\beta,\gamma > 2m$; $q''=24$ edges on the boundary of hexagons and squares relate to shells $\alpha,\beta,4m$, where $\alpha+\beta=2m$; $\alpha,\beta=0$. Atoms inside squares belong to shells $\alpha,\beta,4m$, $\alpha+\beta<2m$, atoms inside hexagons form shells α,β,γ, $\alpha+\beta+\gamma=6m$, $\gamma<4m$.

Each atom of tetrakaidecahedron vertices has 6 nearest neighbors, each of $36(2m-1)$ atoms of edges have 7 nearest neighbors, each of $6(2m-1)^2$ atoms inside squares has 8 nearest neighbors and each of $96m^2-48m+8$ atoms inside hexagons has 9 nearest neighbors. This gives for the number of atoms of a cluster-tetrakaidecahedron n and its surface energy E_{sur}:

$$n=128m^3+60m^2+12m+1,$$
$$E_{sur}=192m^2+60m+6. \qquad (16)$$

Table VI contains these parameters for the first terms of the sequence of clusters-tetrakaidecahedron. Note that these relate to optimal structures of clusters with close packing (compare Tables II and VI).

Consider one more structure of a truncated octahedron which is formed from an octahedron by cutting off 5 atoms near each vertex. Assume that the mth term of the sequence of truncated octahedra is formed from the $(m+1)$-th term of the octahedron sequence. Then the cut-off atoms belong to shells $0,0,2m+2$ and $1,1,2m$. The surface of the obtained figure consists of 6 squares with the side of length 3, and of 8 irregular hexagons. Cutting off of the above atoms decreases the number of cluster atoms of oc-

TABLE V. Parameters of the octahedron cluster.

m	n	E_{sur}	E_{opt}
1	19	54	54
2	85	150	144
3	231	294	291
4	489	486	469
5	891	726	711
6	1469	1014	990

TABLE VI. Parameters of the tetrakaidecadron cluster.

m	n	E_{sur}
1	201	251
2	1289	894
3	4033	1914

TABLE VII. Parameters of the truncated octahedron cluster.

m	n	E_{sur}
1	55	114
2	201	253
3	459	450
4	861	690
5	1439	978
6	2221	1314

TABLE VIII. Asymptotic parameter A for large clusters.

Structure	A
Cubo-octahedron	8,07
Cube	9,52
Octahedron	7,86
Tetrakaidecahedron	7,55
Optimal	$7,62 \pm 0,06$

tahedra by 30 and the cluster surface energy by 36. Thus from formula (15) we have for the cluster parameters:

$$n = 16m^3/3 + 24m^2 + 110m/3 - 11,$$

$$E_{sur} = 24m^2 + 72m + 18. \tag{17}$$

Table VII contains data for the first terms of the sequence for considering truncated octahedra. Note that all clusters except the last one relate to the optimal cluster structure with close packing (see Table II).

Let us consider asymptotic properties of clusters with the structures being considered. We approximate the surface energy of large clusters E_{sur} as a function of a number of cluster atoms n by the dependence:[6]

$$E_{sur} = An^{2/3} \tag{18}$$

and find the values of A for large m of the sequence with the corresponding structure. Table VIII lists these data, and Fig. 7 gives these values for optimal configurations which are obtained as a result of treatment of Table II data for an interval $n = 400$–2000 and use of formula (18). The oscillatory form of this dependence explains the result that the mean value A for the optimal structure is larger than for the tetrakaidecahedron structure. Indeed, the tetrakaidecahedron structure corresponds to some optimal cluster structures with closed shells and the coefficient A is larger for nonclosed cluster shells than for closed ones.

Thus the method being considered allows us to analyze various closed structures of clusters with close packing within the framework of a common scheme. Therefore, this method gives a possibility to compare parameters of different structures and is useful for optimization of cluster parameters.

6. CLUSTERS WITH THE ICOSAHEDRAL STRUCTURE

The interaction potential (4) admits cluster structures for which distances between nearest neighbors are not fixed, but can vary over a certain range near the mean value. The most important of these structures is the icosahedral one[5] because it can provide the maximum number of bonds between atoms. The icosahedron consisting of 13 atoms is represented in Fig. 8, Ref. 45, and the icosahedron containing 55 atoms is given in Fig. 9, Ref. 20. The icosahedron surface consists of 20 regular triangles, and all 12 vertices of the icosahedron are located on a sphere.

At first we consider the simplest cluster-icosahedron consisting of 13 atoms. To construct such an icosahedron let us choose one of the cluster atoms as a center, and locate the other 12 atoms on a sphere of radius R in the following way. Two of these are placed on the sphere poles, i.e. they are located on the line which connects these atoms and passes through the center. The other 10 atoms form two regular pentagons whose planes are perpendicular to this line—the icosahedron axis. The pentagons are inscribed in circles that are sections of planes and the sphere, and the pentagon vertices are rotated by the angle $\pi/5$ against each other. These circles form a cylinder whose axis is the icosahedron axis.
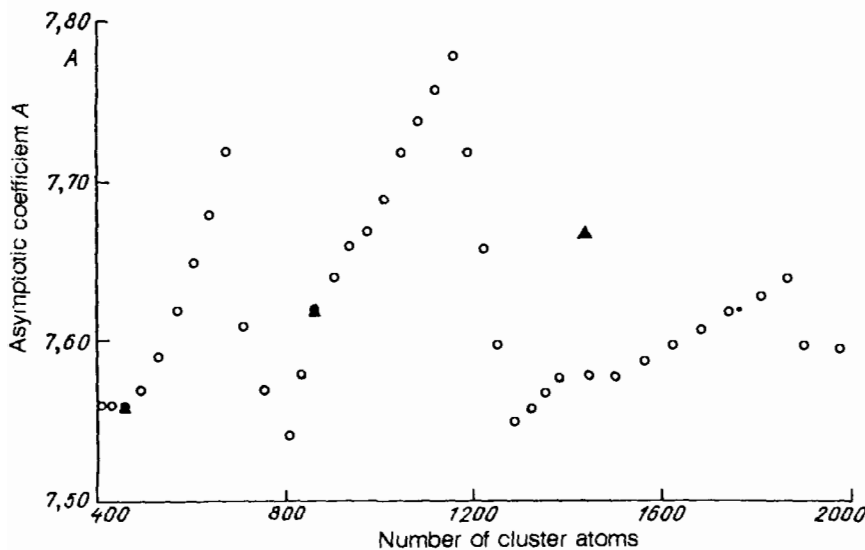

FIG. 7. The asymptotic coefficient A of formula (18) calculated on the basis of Table II data ($\bigcirc$) and for the structure of a truncated octahedron (Table VII) ($\triangle$).
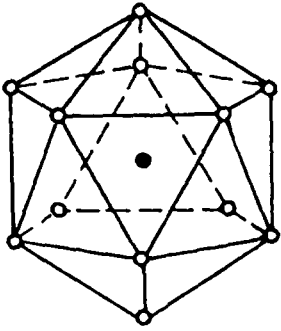
FIG. 8. Icosahedron cluster consisting of 13 atoms.[45] The dark circle relates to the central atom. Lines join surface atoms-nearest neighbors are shown.

Joining the nearest vertices of the icosahedron we obtain 20 regular triangles. This means that the distances between nearest neighbors on the sphere are the same, and each atom has 5 nearest neighbors on the sphere. Nearest neighbors of polar atoms on the sphere are atoms of the nearest pentagon, and each atom of the pentagon has as nearest neighbors on the sphere one atom of the nearest pole, two nearest atoms of its own pentagon and two atoms of the neighboring pentagon.

The distance between nearest neighbors on the sphere of the icosahedron differs a little from the sphere radius, i.e. from the distance between the central and surface atoms. Therefore, strictly speaking, the icosahedron is not a structure with close packing where distances between nearest neighbors are fixed.

The icosahedron has a high symmetry. It is characterized by 6 axes which pass through the center and opposite atoms of the sphere. Rotating through the angle $2\pi/5$ around any of these axes preserves the figure. Besides, the icosahedron is preserved as the result of turning by the angle $\pi/5$ around one of these axes and reflection with respect to the plane which is perpendicular to the axis and passes through the center. One more symmetry of the icosahedron corresponds to the inversion operation $x \leftrightarrows -x$; $y \leftrightarrows -y$; $z \leftrightarrows -z$. And the icosahedron has the symmetry for reflection with respect to the plane which passes
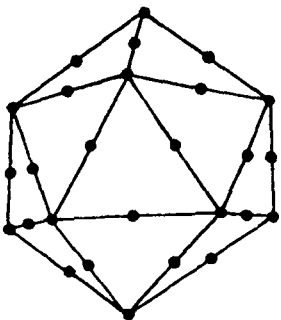

FIG. 9. Icosahedron cluster consisting of 55 atoms and positions of centers of surface atoms.[49]

through a given symmetry axis and two atoms of pentagons. It takes place also for any axis of the icosahedron.

Let us find the relation between the sphere radius and the distance between nearest neighbors on the sphere for the icosahedron. Let R_0 be the distance between nearest neighbors on the sphere whose radius is R and the radius of the cylinder in which the pentagons are inscribed is r. One can obtain the following relations between the icosahedron parameters. The pentagon side length is equal to:

$$R_0 = 2r \sin(\pi/5). \tag{19a}$$

The distance between nearest neighbors that are vertices of different pentagons is:

$$R_0 = \{l^2 + [2r \sin(\pi/10)]\}^{1/2}, \tag{19b}$$

where l is the distance between pentagons. The distance between a pole and an atom of the nearest pentagon equals

$$R_0 = \{r^2 + [r - (l/2)]^2\}^{1/2}. \tag{19c}$$

Moreover, the following relation holds between the sphere radius and the ring radius in which the pentagons are inscribed:

$$R^2 = r^2 + (l/2)^2. \tag{19d}$$

One can see that the first three equations give the relation between the icosahedron parameters, and the fourth equation allows us to check the validity of the icosahedron definition. The first and the second equations give:

$$r = l = 0.851 R_0. \tag{20}$$

From the third equation we have:

$$R = l = 0.951 R_0. \tag{21}$$

The last equation corroborates these relations. Thus, the distance from the center to the icosahedron vertices is approximately 5% less than between the nearest vertices of the icosahedron.

The icosahedron-cluster of 13 atoms under consideration contains 30 bonds of length R_0 and 12 bonds of length R. For comparison note that the cubo-octahedron-cluster consisting of 13 atoms has 36 bonds. It is seen that the icosahedral structure is more favorable among clusters with 13 atoms than structures with close packing and a fixed distance between any nearest neighbors.

Let us consider the following cluster of the icosahedral sequence which consists of 55 atoms (see Fig. 9). 5 atoms of this icosahedron are located on its axis with the distance $R = 0.951 R_0$ between nearest atoms. Twenty atoms form 4 pentagons which are inscribed in a cylinder of radius $r = 0.851 R_0$. Ten atoms form 2 large pentagons which are inscribed in a cylinder of the radius $2r$. The axis of both cylinders is the icosahedron axis, and planes of all pentagons are perpendicular to this axis. Twenty atoms are located at the midpoints of sides of large triangles which are not joined with the icosahedron axis. Relative positions of pentagon atoms of such a cluster are represented in Fig. 10. There is in this figure the developed view of the small cylinder and projections of all pentagon atoms on this cylinder surface. Moreover Fig. 11 contains projections of
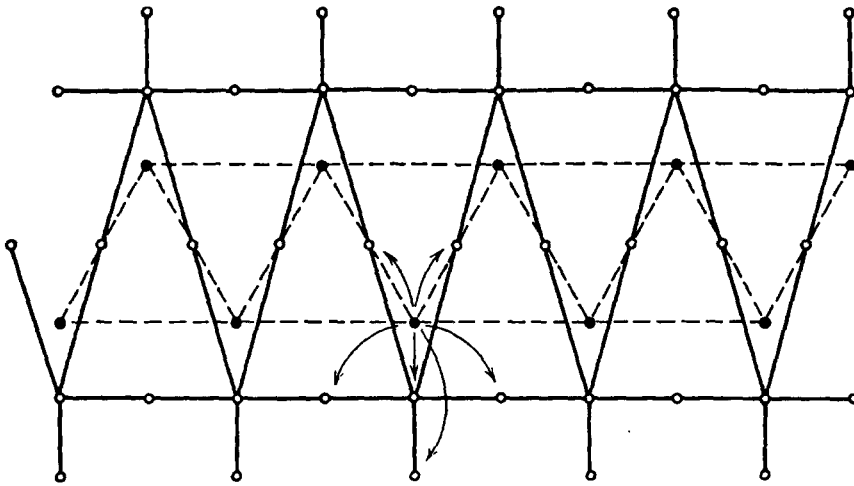
FIG. 10. The developed view of the icosahedron cluster consisting of 55 atoms. This cluster contains a central atom, 12 atoms on the surface of a small sphere, 12 atoms on the surface of a large sphere with twice the radius of the small sphere and 30 atoms at midpoints of lines joining atoms of the large sphere. A developed view of the internal cylinder is given with projection on it of all atoms except those located on the icosahedron axis. Solid lines are sides of large triangles, and dotted lines are sides of small ones. Solid circles are centers of atoms of the external layer, open circles relate to internal atoms, arrows show bonds of one of the atoms.

atoms of the large pentagons and internal atoms of small pentagons onto a plane which is perpendicular to the icosahedron axis.

The icosahedron cluster consisting of 55 atoms has 84 bonds between nearest neighbors with the bond length of $R=0.951R_0$ and 150 bonds between nearest neighbors with the bond length of R_0. From this we have for the total binding energy of atoms in the icosahedron-cluster of 55 atoms neglecting the long-range interaction:

$$E=234D-0.067U''(a)a^2, \qquad (22)$$

where $U''(a)$ is the second derivative of the pair interaction potential at its minimum. In particular, it corresponds to the total binding energy of atoms $229D$ for the Lennard–Jones potential, and the total binding energy of
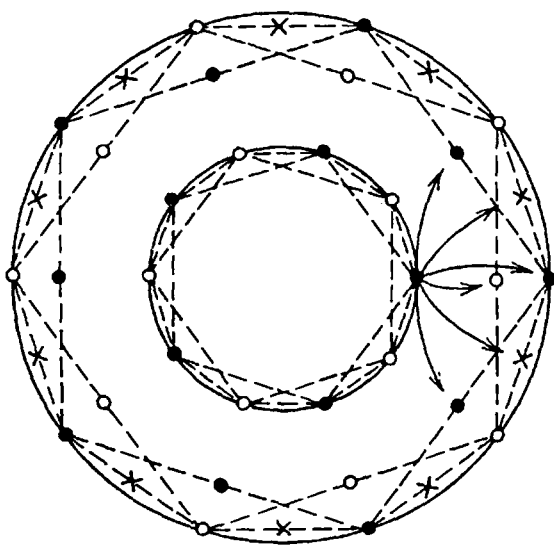

FIG. 11. Projections of the icosahedron cluster consisting of 55 atoms onto a plane which is perpendicular to the icosahedron axis. Atoms on the axis and internal pentagons are excluded from the figure. Crosses correspond to centers of atoms of the central plane, open and solid circles relate to atoms of the lower and upper plane respectively. Dotted lines correspond to sides of triangles, arrows mark bonds for one of the atoms.

atoms is $216D$ for the cubo-octahedron cluster (Table III). It can be seen that the icosahedral structure is more favorable for this cluster than the cubo-octahedral one which is the optimal cluster structure with close packing and $n=55$ (see Table II).

Now using the accumulated experience, construct large icosahedra by taking into account that their surface consists of $s=20$ regular triangles, has $p=12$ vertices and $q=30$ common edges. The first cluster of the icosahedron sequence contains one central atom and $p=12$ atoms-vertices. The edge length of the second cluster of the icosahedron sequence is twice as great as the edge length of the first cluster. Let us locate atoms of the second layer in the vertices of the icosahedron and in midpoints of edges. Thus the second layer contains $\Delta n=p+q=42$ atoms, and the total number of atoms for the second cluster-icosahedron is $n=55$. The third layer has the edge length three times as great as the edge length of the first cluster. This layer contains p atoms as vertices of the figure, $2q$ atoms in edges of the figure and s atoms in midpoints of triangles. Thus this layer contains $\Delta n=p+2q+s=92$ atoms, and the total number of atoms for the third icosahedron cluster is equal to $n=147$.

Continuing this operation, we have that the mth icosahedron cluster has the edge length m times as great as the length of the first one. Dividing each edge into m parts, draw through the formed points lines which are parallel to the sides of triangles. Let us locate atoms in these points and the points of intersections of lines. We obtain a number of atoms at the vertices $p=12$, on the sides of triangles $q(m-1)$ and inside triangles $s(m-1)(m-2)/2$. Thus the mth layer contains $\Delta n=10m^2+2$ atoms. The total number of atoms for the mth icosahedron cluster is equal to:

$$n=10m^3/3+5m^2+11m/3+1. \qquad (23)$$

It can be seen that the number of atoms for the mth icosahedron and cubo-octahedron is the same. This fact simplifies the comparison of parameters for different structures which has been made repeatedly for the pair Lennard–Jones interaction potential Refs. 16, and 19–21.

Let us evaluate the binding energy of atoms for the icosahedral clusters taking into account the short-range interaction between atoms—nearest neighbors only. We have that each surface atom placed at a vertex of the icosahedron has 1 bond of length R and 5 bonds of length R_0, each edge atom has 2 bonds of length R and 6 bonds of length R_0, and the surface atoms inside triangles have 3 bonds of length R and 6 bonds of length R_0. Summarizing, we found that addition of the mth icosahedron layer increases the binding energy of cluster atoms by the value

$$\Delta E = p\left(\varepsilon_1 + \frac{5}{2}\varepsilon_2\right) + q(m-1)(2\varepsilon_1 + 3\varepsilon_2) + \frac{1}{2}s(m-1)$$

$$\times (m-2)(3\varepsilon_1 + 3\varepsilon_2)$$

$$= \varepsilon_1(30m^2 - 30m + 12) + \varepsilon_2 \cdot 30m^2, \qquad (24)$$

where $\varepsilon_1 = -U(R)$, $\varepsilon_2 = -U(R_0)$—the binding energies of two atoms for distances between them R and R_0 correspondingly. We take into account that bonds of length R_0 connect surface atoms, and such bonds are repeated twice as the result of addition of a new layer. Thus the total binding energy of atoms of the icosahedron is equal to:

$$E = 10m^3(\varepsilon_1 + \varepsilon_2) + 15m^2\varepsilon_2 + m(2\varepsilon_1 + 5\varepsilon_2). \qquad (25)$$

Let us illustrate the method of determination of the total cluster energy on the basis of formula (25). Transform formula (25) to the form:

$$E = A\varepsilon_1 + B\varepsilon_2 = -AU(R) - BU(R_0), \qquad (26)$$

where $A = 10m^3 + 2m$, $B = 10m^3 + 15m^2 + 5m$. Choose the optimal relation between the parameters R, R_0 and R_e—the equilibrium distance between atoms of the diatomic molecule. Expanding the interaction potential near the equilibrium distance, choose the parameters R, R_0 such that the total binding energy has a minimum. It gives the following expressions for optimal distances:

$$R_0 = a + \frac{0.049Aa}{0.951A + B}, \quad R = a - \frac{0.049Ba}{0.951A + B} \qquad (27)$$

and the optimal binding energy of atoms in the cluster is equal to:

$$E = (A + B) - U''(a)a^2 \frac{0.049^2 AB(A + B)}{2(0.951A + B)^2}. \qquad (28)$$

The obtained expressions allow us to understand the behavior of the cluster energy for large clusters. Then $A = B = 10m^3$ and we have from formula (28) for the total energy of the cluster–icosahedron:

$$E = (20 - 0.0063U''(a)a^2)m^3 + 15m^2. \qquad (29)$$

Comparing it with the total energy of the cubo-octahedral cluster, we have that an internal atom of any structure has 12 nearest neighbors, but the distances between nearest neighbors are equal to the optimal one for the cubo-octahedral structure and differ a little from the optimal one for the icosahedral structure. Therefore, the coefficient for the term m^3 is a little higher for clusters with close packing than for the icosahedron structure. On the other hand,

m	n	Number of bonds	E	E_{opt}
1	13	42	41,2	36
2	55	234	229	216
3	147	696	681	662
4	309	1548	1514	1492
5	561	2910	2846	2835
6	923	4902	4793	4809
7	1415	7644	7474	7527
8	2057	11256	11005	11116

surface atoms of the icosahedron have more nearest neighbors than in the case of structures with close packing. From this it follows that the icosahedron structure is the optimal one for not very large clusters, and large clusters must have the structure with close packing.

The transition from one structure to other one is expected at $n \sim 1000$. Table IX lists the total binding energies for icosahedra in the case of the truncated Lennard–Jones interaction potential if only the interaction of nearest neighbors is taken into account. As can be seen from Table IX, the binding energies of clusters with the icosahedral structure E and with close packing E_{opt} are compared at $n \sim 1000$.

Note that inclusion of a long-range interaction between cluster atoms increases typical values of n up to which the icosahedral structure is the optimal one. A long-range interaction is stronger for the icosahedron structure than for structures with close packing because of its higher density. For example, for large clusters the radius of the sphere on which vertices of structures are placed are higher by 2.4% for the icosahedral structure than for the structure with close packing. Add to this that according to the experimental studies (Refs. 8, 10, 16, 19, 46–48) of rare gas clusters by the method of electron diffraction by cluster beams, neutral clusters of rare gases have the icosahedral structure for $n < 1000$ and the structure with close packing is realized for n of a few thousand. Investigations of charged clusters of rare gases[49-56] have shown that the magic numbers of clusters depend on the cluster type and conditions of cluster formation. But for all cases of studies the icosahedral structure of clusters corresponds to observing magic numbers for $n < 1000$.

7. DISTRIBUTIONS OF CLUSTER ATOMS AMONG SHELLS

Analyzing the properties of large clusters, we compare these with properties of macroscopic particles. Experience with such a comparison shows a correspondence in cases of some properties and a lack of correspondence in other cases. Further we consider this question for distributions of cluster atoms among cluster shells. Because of the high symmetry of a cluster with close packing, each cluster shell contains many (6–48) atoms. If the cluster under consideration forms a symmetric figure or is close to it, the number of atoms in the same state becomes even greater. Further we construct the distribution of cluster atoms among shells using the macroscopic concept of the cluster with

close packing and check the validity of this concept. Then one can use the Fermi–Dirac formula for occupation numbers:[57]

$$q_{nk}=n_k\{1+\exp[(\varepsilon_k-\mu)/T]\}^{-1}. \tag{30}$$

Here n_k is the number of atoms on the kth shell, q_{nk} is the optimal number of atoms on this shell at a total number of cluster atoms n, ε_k is the binding energy of the atom for this shell, μ is the chemical potential of the cluster which satisfies the relation:

$$n=\sum_k q_{nk}=\sum_k n_k\{1+\exp[(\varepsilon_k-\mu)/T]\}^{-1}. \tag{31}$$

Assuming the chemical potential to be a smooth function of n ($|\mu_{n+1}-\mu_n|\ll\mu_n$), we have:

$$\mu_{n+1}=\mu_n+d\mu_n/dn.$$

In this case by taking the derivative of the relation (31) we obtain for the cohesive energy of the cluster which is the mean energy of a released atom:

$$\varepsilon_n=d\sum\varepsilon_k q_{nk}/dn$$

$$=\sum_k\varepsilon_k q_{nk}(n_k-q_{nk})n_k^{-1}\left[\sum_k q_{nk}(n_k-q_{nk})n_k^{-1}\right]^{-1}. \tag{32}$$

It may be seen that free and closed shells give a small contribution to the cohesive energy. Therefore, analyzing the distribution of atoms among cluster shells, we must concentrate the main attention on shells being filled.

To check the validity of the Fermi–Dirac formula for considering clusters we compare its result with the accurate one. Use a simplified cluster model according to which the cluster under consideration has only two shells that are not free or closed. Label the number of states for the lower shell by l, the number of states for the upper shell by m, the energy difference between the upper and lower shells as ε. The equation for the chemical potential in accordance with the Fermi–Dirac formula (30) has the form:

$$n=l/(1+X)+m/(1+XY), \tag{33}$$

where $X=\exp[(\varepsilon_l-\mu)/T]$, ε_l is the energy of the lower shell, $Y=\exp(\varepsilon/T)$. The solution of this equation allows us to find the distribution of atoms among shells within the framework of the Fermi–Dirac approximation.

Use the simplified cluster model for the accurate distribution of atoms among shells. The probability to have q atoms on the upper shell has the form:

$$W_q=C_l^{n-q}C_m^q Y^{-q}/Z, \tag{34}$$

where C_l^q is the number of combinations of l items taken q at a time, and the partition function is equal to:

$$Z=\sum_{q=0}^{\min(l,n)}C_l^{n-q}C_m^q Y^{-q}. \tag{35}$$

It gives for the cluster excitation energy:

TABLE X.

n	23	24	25	26
Z, 10^7	11,0	6,6	3,6	1,8
$\bar{q}_n$	8,0 (8,1)	8,5 (8,7)	9,1 (9,2)	9,7 (9,8)
Δq_n	1,61	1,70	1,72	1,77
$\Delta q_n/q_n^{1/2}$	0,57	0,58	0,57	0,57
$\bar{q}_n-\bar{q}_{n-1}$		0,55 (0,56)	0,58 (0,58)	0,62 (0,60)

$$E_n=\varepsilon\bar{q}_n=\sum_q qC_l^{n-q}C_m^q Y^{-q}/Z, \tag{36}$$

where $\bar{q}_n$ is the mean number of atoms on the upper shell. This value is similar to

$$E_n=m\varepsilon/(1+XY), \tag{37}$$

which relates to the Fermi–Dirac distribution.

Compare these two expressions for clusters with close packing within the framework of the above simplified scheme. Choose the shell 037 as the lower shell of the cluster (see Table II), and the group of shells 008, 118, 028 as the upper shell. The cluster growth at zero temperature is accompanied by simultaneous occupation of these shells. Averaging over the parameters of these shells, we have for the parameters of the model under consideration:

$$l=24, \quad m=54, \quad \varepsilon_l=-6D, \quad \varepsilon=2D/3.$$

Table X lists data which characterizes the distribution of atoms among cluster shells at the temperature $T=0.3D$ (i.e. $Y=9.2$). Values of parameters which correspond to the Fermi–Dirac approximation are given in Table X in parentheses. It can be seen that the error due to using the Fermi–Dirac approximation does not exceed several percent. Figure 12 gives distributions according to occupation numbers evaluated on the basis of formula (31). From this one can determine the standard deviation:

$$\Delta q_n^2=q_n^{-2}-(\bar{q}_n)^2.$$

According to data in Table X where these values are given the ratio $\Delta q_n/q_n^{1/2}$ practically does not depend on n.

From Table X it follows that the partition function in the present case is large $Z\sim10^7-10^8$. It means that the effective number of cluster states is large too and justifies the use of the Fermi–Dirac approximation for this case. Moreover, the average excitation energy of clusters lies in the interval $5D-6D$, i.e. significantly exceeds the cluster thermal energy $T=0.3D$. This also confirms the validity of statistical methods.

But there is an ultimate problem because the energy parameters of atoms for each shell ε_k depend on the occupation of neighboring shells. One can expect that for a real distribution of atoms among shells the mean values of ε_k change but little for the most probable distributions of atoms among shells. This allows us to construct a perturbation theory whose zero order approximation is the distribution of atoms among shells at zero temperature. One can obtain from this mean values of ε_k which are used for the first order approximation of the pertubation theory. Such a
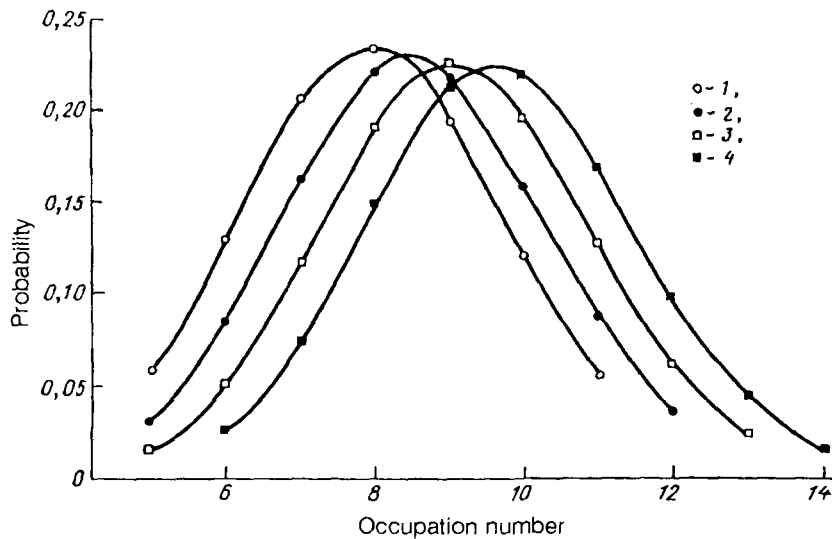
FIG. 12. The distribution of clusters with close packing consisting of $807+n$ atoms with respect to the number of atoms in the upper shell at the temperature of $0.3D$: ○—$n=23$; ●—$n=24$; □—$n=25$; ■—$n=26$.

pertubation theory works the better the nearer is the cluster structure to the symmetric one for which any shell is either occupied or free.

Figure 13 gives the cohesive energy of clusters with close packing as a function of the number of cluster atoms. It corroborates the conclusion that a large cluster differs from a macroscopic particle. An increase of the temperature smooths out the dependence of cluster energy parameters on the number of atoms in it, but this dependence does not coincide with that which corresponds to macroscopic particles.

Thus a cluster with close packing is a convenient model which allows one to analyze the validity of a macroscopic description for distributions of atoms in a cluster. The validity of the Fermi–Dirac distribution for clusters with close packing is explained by the high cluster symmetry. It leads to a large number of atoms in the same states. It holds not only for clusters with close packing, but also in the case of other symmetric clusters including clusters with the icosahedral structure.

8. LARGE SYMMETRIC CLUSTERS AND FLAT SURFACES

The main property of clusters relates to the large specific area of their surface. Therefore, one can expect an analogy between cluster and surface properties. Properties of the symmetric clusters under consideration must be found in greater correspondence with properties of surface because they have flat boundaries. Atoms on these boundaries are found to be under the same conditions as atoms of a macroscopic surface. Therefore this analogy deserves attention.

Add to this that the Fermi–Dirac approximation is more valid for symmetric clusters. Indeed, the maximum number of atoms on one cluster shell is equal to 48, but a flat surface of symmetric clusters can contain a much greater number of atoms with identical parameters. For example, the tetrakaidecahedron—a cluster with $m=2$ which consists of 1289 atoms has 24 vertex atoms with the binding energy $\varepsilon=6$, 108 edge atoms with $\varepsilon=7$, 54 atoms inside surface squares with $\varepsilon=8$, and 296 atoms inside
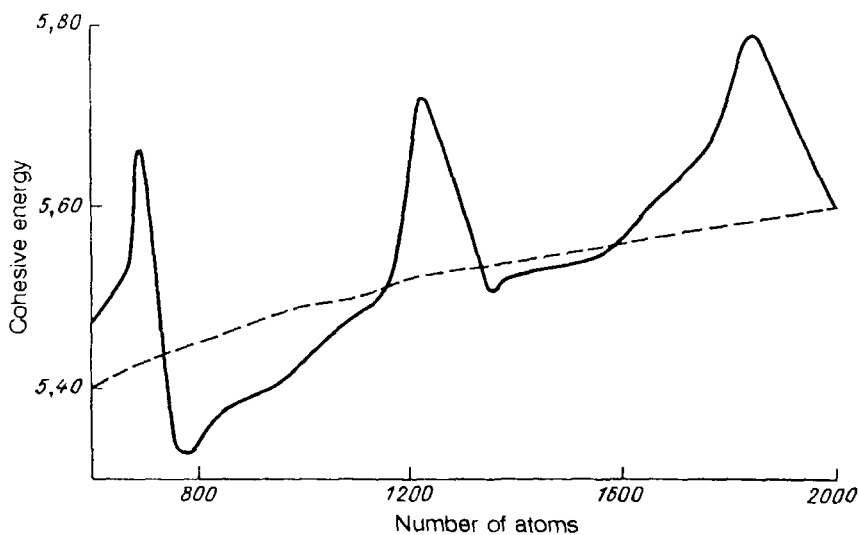

FIG. 13. The cohesive energy of clusters with close packing at $T=0.3D$. The dotted line corresponds to a macroscopic particle.

surface hexagons with $\varepsilon = 9$. Therefore the Fermi-Dirac approximation is valid for cluster structures which are close to symmetric ones.

Let us consider such a case assuming the number of excited atoms from the cluster surface to be relatively small. Divide the surface atoms into two groups. Label the atoms of the cluster surface by the subscript i and the atoms of excited shells by the subscript k. The condition of a small number of excitations means that $\exp[(\varepsilon_k - \mu)/T] \ll 1$ and $\exp[(\varepsilon_i - \mu)/T] \gg 1$. Using these conditions in the Fermi–Dirac formula (30) we obtain:

$$\Delta n = \sum_i n_i \exp(-\varepsilon_i/T) X - \left[\sum_k n_k \exp(\varepsilon_k/T)/X \right], \quad (38)$$

where

$$\Delta n = n - \sum_k n_k, \quad X = \exp(\mu/T).$$

This gives for the chemical potential of the cluster:

$$\mu = T \ln \left\{ \frac{\Delta n}{2a} + \left[\left(\frac{\Delta n}{2a} \right)^2 + \frac{b}{a} \right]^{1/2} \right\}, \quad (39)$$

where

$$a = \sum_i n_i \exp(-\varepsilon_i/T), \quad b = \sum_k n_k \exp(\varepsilon_k/T).$$

Here n_i is the total number of possible excited states.

Let us go to the macroscopic limit assuming

$$\Delta n \ll (a/b)^{1/2} = 1/X. \quad (40)$$

Then the numbers of vacancies and excitations are equal to each other and are $\sqrt{ab}$. As can be seen, in this case a cluster is like a semiconductor with a small density of free electrons with atoms of the cluster playing the role of electrons of the semiconductor. Such a semiconductor has the Fermi level in the middle of a forbidden band.[1] Then we have for the cluster chemical potential $\mu = 6D$ with an accuracy up to thermal energy.

It is possible to obtain this result in a simple way by using the symmetry of the problem. Indeed, let us take a unit of a flat surface and assume the surface to be entirely covered by atoms at zero temperature. Then the numbers of vacancies and excitations are the same at a finite temperature, and the system is symmetrical with respect to a replacement of vacancies by excitations. From this it follows that the chemical potential of such a surface and the cluster cohesive energy are equal to $6D$. This coincides with the result of Ref. 24 for the cohesive energy of a flat macroscopic surface which was obtained for a system of surface atoms with a short-range interaction and a certain structure of this surface. Note that it is not important that the atoms must entirely cover a macroscopic surface at zero temperature because in the opposite case transitional zones exist over a small part of the surface area.

Let us obtain the criterion that the surface of a symmetric cluster is like a macroscopic surface. Assume the number of cluster atoms to be close to that of a symmetric figure and the distribution of cluster atoms to be close to

that of the symmetric structure. Then cluster vertices and edges play a role of transitional zones of a macroscopic surface. Therefore the possibility to use for the cluster parameters of a macroscopic surface demands the neglect of vertex and edge atoms compared with surface ones. This corresponds to the criterion:

$$n_{\text{sur}} \exp(-\Delta\varepsilon/T) \gg n, \quad (41)$$

where n_{sur} is the number of atoms situated on the cluster flat surfaces, n' is the number of vertex and edge atoms, $\Delta\varepsilon$ is the difference in the binding energy for atoms situated on cluster surfaces and on its vertices or edges.

Consider as an example the case of the cluster-tetraikaidecadron consisting of 1289 atoms at the crystal melting point $T = 0.58D$. Then the small parameter corresponding to the criterion (41) has the form:

$$\alpha = [n_p + n_q \exp(-D/T)]/[n_r \exp(-2D/T)$$
$$+ n_s \exp(-3D/T)], \quad (42)$$

where n_p, n_q, n_r, and n_s are respectively numbers of cluster atoms that are located on the vertices, edges, surfaces of squares and surfaces of hexagons. From this we have for the cluster with $m = 2$ consisting of 1289 atoms at the crystal melting point $T = 0.58D$ $\alpha = 13$, i.e. this cluster does not have an analogy with a macroscopic surface. An asymptotic expression for the small parameter in the limit $m \to \infty$ has the form at the crystal melting point $T = 0.58D$:

$$\alpha = 2.7/m = 14/n^{1/3}.$$

At this temperature the cluster surface becomes identical with a macroscopic surface if the number of cluster atoms is of the order of 10^4. The smaller is the temperature, the larger are cluster sizes demanded for this transition.

Let us analyze the correspondence between large clusters and a macroscopic surface in another way. The mean cohesive atom energy for a macroscopic flat surface is equal to:

$$\varepsilon = 6D. \quad (43)$$

This is the asymptotic limit $n \to \infty$ for clusters with close packing. Taking into account the next term in the expansion of the small parameter $n^{-1/3}$ leads to a macroscopic cluster model—the liquid drop model. Then in accordance with formulae (8), (18) the mean cohesive energy is equal to:

$$\varepsilon = dE/dn = 6D - 2AD/3n^{1/3}, \quad (44)$$

where E is the total binding energy of atoms in the cluster. This formula is transformed for the cluster with close packing to the form:

$$\varepsilon = 6D - 5.1D/n^{1/3}. \quad (45)$$

Note that the mean cluster cohesive energy is a little less than the cluster sublimation energy related to one atom which is equal to:

$$\varepsilon_{\text{sub}} = E/n = 6D - 7.6D/n^{1/3}. \quad (46)$$

For the truncated Lennard–Jones interaction potential without a long-range interaction the sublimation energy of
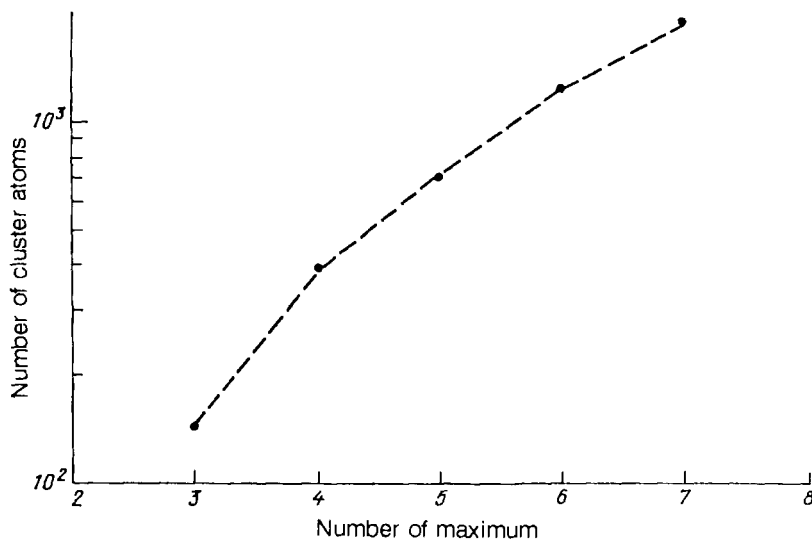
FIG. 14. Positions of maxima for the cohesive energy as a function of the number of cluster atoms. The dotted line relates to the dependence $\varepsilon(n) = 5m^3 + 4m^2$.

a large cluster with the icosahedral structure is given by the expression which follows from formulae (23), (29):

$$\varepsilon_{\text{sub}} = E/n = 5.86D - 6.55D/n^{1/3}. \tag{47}$$

It is of interest to compare this expression with that corresponding to the Lennard–Jones interaction potential of atoms taking into account a long-range interaction. From treatment of the data of Ref. 21 we have the asymptotic expressions for the sublimation energy of clusters with the cubo-octahedral structure:

$$\varepsilon_{\text{sub}} = E/n = 8.41D - 12.7D/n^{1/3} \tag{48}$$

and with the icosahedral structure:

$$\varepsilon_{\text{sub}} = E/n = 8.57D - 15.6D/n^{1/3}. \tag{49}$$

Note that the close values of coefficients of formulae (48), (49) are obtained in Ref. 16 by approximation of numerical values in some range of n. The asymptotic value of the first coefficient, i.e. the sublimation energy of the crystal per one atom for the Lennard–Jones interaction potential is equal to $8.61D$ (Ref. 1). This value for the lattice with close packing refers to the cubo-octahedral cluster structure. The degree of correspondence of this value to the coefficient of formula (48) characterizes the accuracy of formulae (48), (49).

Figure 13 gives the average cohesive energy of the cluster with close packing at the temperature $T = 0.3D$. One can seen that the cohesive energy oscillates as a function of n and differs from that corresponding to a macroscopic particle [formula (45)]. With cluster increase the amplitude of oscillations must decrease and the cohesive energy $\varepsilon(n)$ will tend to the macroscopic limit.

Note that according to Fig. 13 and the data of Table II maxima of the cluster cohesive energy correspond to attachment of blocks with shells 0, β, β, to the cluster. Minima of the cluster cohesive energy correspond to attachment of blocks which include shells 0, β, γ, where $\beta = 0$ or 1 or an attaching block is started from a shell α, β, γ, where $\alpha \approx \beta \approx \gamma$. With increase of cluster size these blocks are increased and the binding energy difference for neigh-

boring blocks falls. Moreover, neighboring blocks grow independently for clusters of large size, and the function $\varepsilon(n)$ becomes smooth. Then the cluster becomes similar to a macroscopic particle.

Denote positions of maxima of the cohesive energy by n_{max} and assume these to correspond to half-occupied blocks with maximum binding energies of atoms at zero temperature. Figure 14 gives some values of n_{max}. The corresponding blocks contain a shell 0, m, m whose atoms are vertices of cubo-octahedra, but the optimal sequence of cluster growth differs from the cubo-octahedral one. Positions of maxima of $\varepsilon(n)$ in Fig. 14 are compared with the dependence

$$n_{\text{max}} = 5m^3 + 4m^2, \tag{50}$$

(m is the maximum number) which is the optimal one for not too great values of m.

Thus $\varepsilon(n)$ has an oscillatory character for $n \sim 1000$, and oscillations are important up to $n \sim 10^4$. Such a form of the cluster cohesive energy influences the character of the cluster growth. In particular, the classical theory of homogeneous condensation[65-71] which is based on the macroscopic drop model for clusters-condensation nuclei-must be changed taking into account the real form of $\varepsilon(n)$. Indeed, intermediate products of the process are clusters for which the dependence $\varepsilon(n)$ differs from that which corresponds to a macroscopic drop.

Thus the analysis of clusters with close packing and comparison of these with macroscopic particles leads to the following conclusions. First, as a system of many bound atoms with a high symmetry such a cluster admits a macroscopic description for distributions of atoms in clusters on the basis of the Fermi–Dirac distribution. Second, the cohesive energy of a cluster is a nonmonotonic function of n, in contrast to a macroscopic particle. Third, if the number of cluster atoms is close to the number of atoms of symmetric structures, the majority of the surface atoms of a close-packed cluster are located at not too great a temperature on the flat surfaces of the structure. Nevertheless,
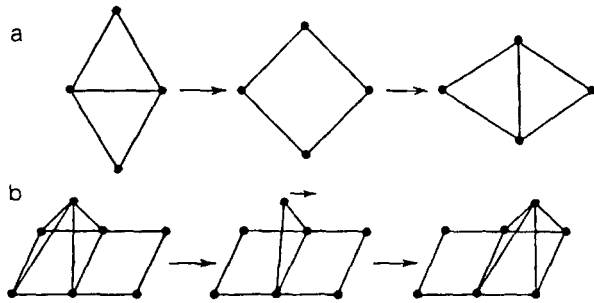
FIG. 15. Processes of the structure transitions between symmetric states of atom systems. a) DSD-process; b) EB-process.

the behavior of a cluster surface differs from the behavior of a macroscopic surface up to $\sim 10^4$ atoms in the cluster.

9. SOLID-LIQUID PHASE TRANSITION

The solid-liquid phase transition is the principal problem of physics of condensed systems.[71] Clusters, and especially their symmetric structures can be useful for an analysis of this problem. The phase transition starts from the surface,[72] and clusters as systems with a large specific area of the surface give some information for this process. Experimental[73-76] and theoretical[77-89] studies of phase transitions for clusters extend our knowledge of this process.

We note that systems of bound atoms with a short-range interaction are suitable systems for understanding the nature of phase transitions due to the high symmetry and simplicity of systems with close packing. Moreover, condensed inert gases are such systems, and existing information about the phase transition of condensed inert gases also helps to understand this problem. Main results for physics of the phenomenon are obtained on the basis of numerical methods of molecular dynamics, and the analysis of the phase transition by such methods is the more detailed the smaller is the number of atoms in the system. Therefore, the phase transition for clusters can be studied in greater detail than for macroscopic systems.

The nature of the phase transition for clusters with a short-range interaction depends on filling the last cluster shell. If the cluster shell is not filled, there is a finite number of states of the cluster with maximum binding energy of atoms. These states relate to different configurations of

atoms, and transitions from one of these states to another are accompanied by atom transitions to new sites in the cluster. Thus, for unfilled cluster shells free movement of atoms of this shell between their sites can take place at low temperatures and small cluster excitations.

There are two types of atom displacement in this case which lead to a change of atom configurations (see Fig. 15). The first of these is the DSD-process[70] (diamond-square-diamond). As a result of this process, the bond passes from one pair of atoms to another one. Usually this process takes place for carbon compounds.[91,92] The other type of the bond transition is called the EB-process (edge-bridging).[93] Then some bonds of the migrating atom are broken, and it rotates on the unbroken bonds to a new site which is symmetrical with respect to the initial one. The final atom state is characterized by the same number of bonds as the initial one. The EB-process of atom displacements relates to systems of atoms with a short-range interaction, in particular, to condensed inert gases.[94-96]

The phase transition of clusters with an unfilled external shell[94-96] can be an analog of the phase transition of an unfilled macroscopic surface. For investigation of the phase transition of macroscopic condensed systems with a short-range interaction it is necessary to use as an analog the symmetrical clusters with filled layers considered above. Then it is of interest for the phase transition of condensed inert gases to consider first of all the closed icosahedral structures, because closed clusters with such a structure have a maximum binding energy.

The peculiarity of the cluster phase transition is determined by the different binding energy of atoms of external and internal shells. Therefore, the phase transition for internal and surface atoms must be observed at different temperatures. As an illustration of this statement, Fig. 16 gives the nature of atom movements in a Si-cluster.[81] Atom trajectories for long times are shown in this figure. If atoms vibrate near the equilibrium positions, their trajectories have the form of smeared out points. If atoms can change their positions, the entire region which joins the equilibrium atom positions is smeared out. As can be seen from Fig. 16, surface atoms can change their positions under the conditions being discussed and this corresponds to the liquid state, while internal atoms are fixed in the lattice nodes and this corresponds to the crystal state.

Figure 17 (Refs. 86, 87) gives another example of this kind and refers to the Ar_{147} cluster which at zero temperature has the icosahedral structure with three filled layers.
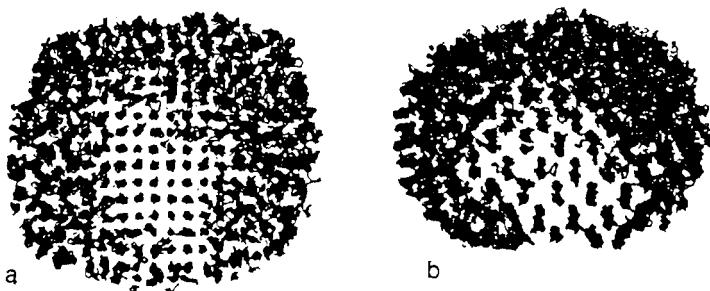

FIG. 16. Space trajectories of atoms for a Si-cluster consisting of 1024 atoms.[81] Slices of the cluster are shown.
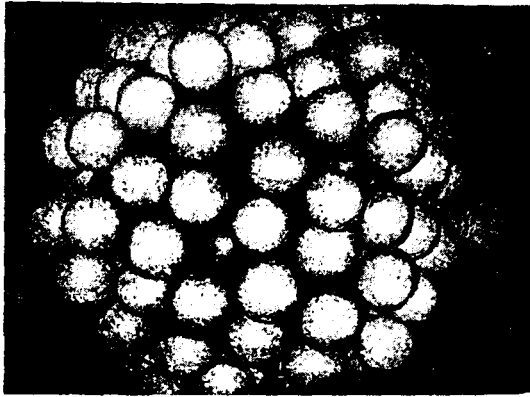
FIG. 17. A snapshot of the cluster Ar_{147} in which atoms are modeled by balls.[86,87]
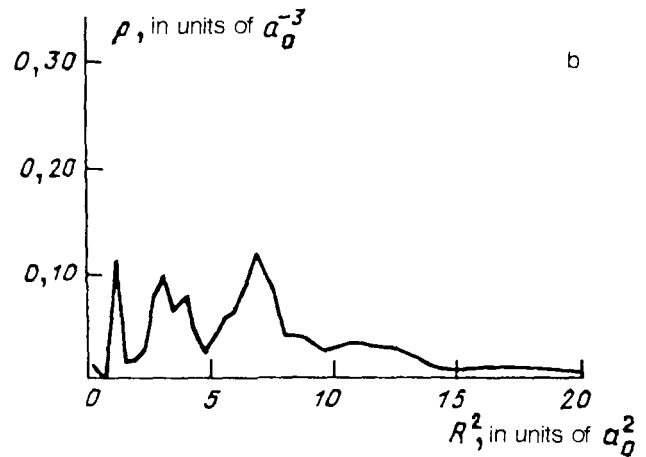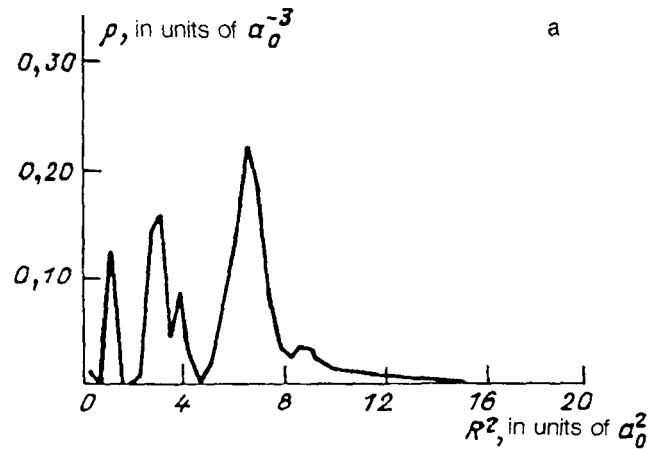

FIG. 18. The atom density of Ar_{147} as a function of the square of the distance from the central atoms near the melting point of the surface layer (38 K).[86,87] a) The solid state of the surface layer; b) the liquid state of the surface layer.

The upper layer becomes liquid under the above conditions, and the internal ones are solid. The atom configuration in the cluster is calculated on the basis of methods of molecular dynamics, and the Lennard–Jones pair interaction potential for atoms is used.

Let us consider the special features of the phase transition which follow from studies of Ar-clusters.[86-90] The conclusion of these studies is that the phase transition of surface atoms does not consist in a random movement of atoms which leads to an amorphous surface of the surface layer. On the contrary, the strong interaction between neighboring atoms is preserved. But the collective movement of surface atoms attains high amplitudes at the phase transition, and this causes ejection of some surface atoms out of the layer. They become attached to a cluster surface and "float" on it. They can return to the surface layer, and then other surface atoms become floating. Thus, the phase transition is explained not by transitions of individual atoms, but by special features collective movements of atoms.

Figure 18 contains the atom distribution in Ar_{147} for the liquid and solid state of the surface layer at the melting point.[86,87] As can be seen, the phase transition is accompanied by displacement of some surface atoms into the next free layer. Then the distribution of internal changes small. The temperature dependence for some parameters of the Ar_{55} cluster is given in Fig. 19 (Ref. 88) near the melting point of the surface layer.

The main special feature of the cluster phase transition is that it has a range of temperatures in contrast to macroscopic systems where the phase transition takes place at a fixed temperature. Therefore the coexistence of liquid and solid phases is possible in a cluster.[90-93] Indeed, in accordance with (Refs. 90–93) introduce the ratio of the probabilities of liquid and solid phases of the cluster in the form $K = \exp(-\Delta F/T)$, where $\Delta F = n\Delta\mu$ is the difference between the free energies of the liquid and solid phases, $\Delta\mu$ is the difference between the chemical potentials for these phases, and n is the number of atoms in the cluster. Assuming $\Delta\mu = (\partial\Delta\mu/\partial T)(T - T_c)$, where T_c is the temperature of the phase transition, we obtain the following ex-

pression for the probability for the cluster to be in the liquid state:

$$w_{liq} = 1 + \exp\left[n\frac{\partial\Delta u}{\partial T}(T - T_c)T^{-1}\right].$$

The transition range is the narrower the larger is n. For a macroscopic system ($n \to \infty$) w_{liq} is a step-function of the temperature, but for a cluster the transition range is characterized by a finite width. Solid and liquid phases coexist in this range.

We give some estimates on the basis of numerical results obtained in Refs. 86–90 for Ar_{55} and Ar_{147} clusters. Note that in this case as in the case of a macroscopic system with a short-range interaction of atoms we have for the melting point:

$$T_c/\varepsilon = 0.04-0.05.$$

Here T_c is the melting point, ε is the energy which is spent on formation of one vacancy in the system. For the surface of clusters this value is equal to the cluster cohesive energy, and in the case of the Lennard–Jones interaction it is equal to $7.04D$ for Ar_{55} and $7.19D$ for Ar_{147} (Ref. 15).
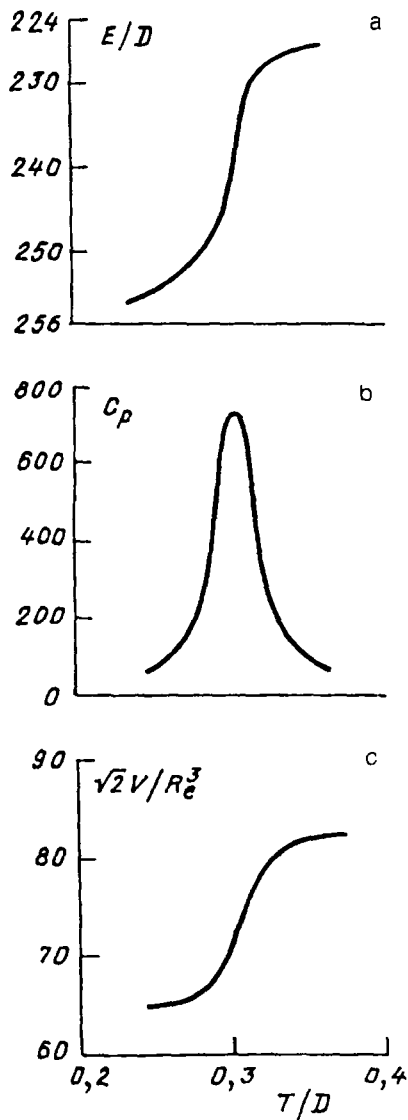
Figure (left column)

a

E/D

224
230
240
250
256

b

C_p

800
600
400
200
0

c

$\sqrt{2}\,V/R_c^3$

90

80

70

60

0,2   0,3   0,4

T/D

FIG. 19. Parameters of the Ar_{55} cluster near the melting point for the surface layer in absence of external pressure.[88] a) The total binding energy E of atoms (in units of D); b) the heat capacity C_p (dimensionless); c) the volume occupied by the cluster (in units of $R_c^3/\sqrt{2}$).

Let us estimate the equilibrium number of vacancies for the crystal state of the Ar_{55} cluster at the phase transition temperature by assuming that it has the icosahedral structure. For simplicity we use the parameters of the truncated Lennard–Jones interaction potential without its long-range part and neglect small difference from the equilibrium distance for nearest neighbors in the icosahedron. This gives that the Ar_{55} cluster contains 13 atoms with the binding energy of $12D$, 30 atoms with the binding energy of $8D$ and 12 atoms with the binding energy of $6D$. In addition, in the unfilled layer there are 20 states with the binding energy of $3D$, 20 states with the binding energy of $2D$ and 12 states with the binding energy of D. Then on the basis of formula (39) we obtain for the cluster chemical potential $\mu = -4.65D$ at the cluster melting point $T = 0.3D$, and the average number of vacancies formed at

the vertices of the cluster at this temperature is equal to 0.13. Taking the long-range interaction into account leads to an increase of this value.

The above estimates contradict the results of computer modeling of this cluster by methods of molecular dynamics because the phase transition for the cluster surface layer takes place at the above temperature and causes the formation of several vacancies. Understanding the reason for this contradiction will allow us to elucidate the nature of the phase transition. Note that application of the Fermi–Dirac distribution for considering a solid cluster is valid because cluster shells are filled and the excitation probability is small. Therefore the used binding energies are accurate, and we must look for the contradiction in neglecting atom vibrations. But the vibrational movement of an individual atom is not essential in this case. Indeed, the binding energy of atoms in the Lennard–Jones cluster at zero temperature is equal to $279D$ (Refs. 15, 16, and 21) while the phase transition of surface atoms corresponds to the binding energy of atoms of approximately $255D$ (see Fig. 19), i.e. the vibrational energy of cluster atoms does not exceed 10% of the total binding energy of the cluster.

Thus vibrations of individual atoms do not influence the cluster behavior. It follows from this that the phase transition can be associated with a nonlinear interaction of collective vibrations of atoms. This is the conclusion of Refs. 86–88 on the basis of numerical modeling of the parameters for the Ar_{147} cluster. Then the question arises as to why a strong interaction of vibrations takes place at small amplitudes of vibration. We note that a Lennard–Jones cluster consisting of 55 atoms with the cubo-octahedral structure has at zero temperature the binding energy of atoms of $268D$ while the phase transition corresponds to the binding energy of atoms of $255D$, i.e. the cubo-octahedral structure can be excited at the temperature of the phase transition. Interaction between the icosahedral and cubo-octahedral structures can provide a nonlinear interaction of vibrations. It relates to symmetrical vibrations in which all cluster atoms partake, and this interaction can lead to a strong redistribution of the energy between degrees of freedom.

Thus the analysis of the phase transition allows us to understand in detail the nature of the phenomenon and the character of melting for surface and internal cluster layers. The dependence of the phenomenon on cluster sizes leads to the above peculiarity of the cluster phase transition. In a macroscopic system the transition from one phase to the other one takes place at a fixed temperature and is accompanied by a change of the internal energy of the system. In clusters this transition takes place in a certain range of temperatures, and the concept of the point of the phase transition must be extended to an interval. We note the methodological side of the problem. The analysis of the phase transition by using molecular dynamics methods becomes more accessible for clusters. Therefore it can be used for understanding the phase transition of macroscopic systems.

Analyzing the phase transition of macroscopic systems, consider the popular model of Stillinger and

TABLE XI. Parameters of the phase transition for condensed inert gases.

Parameter	Ne	Ar	Kr	Xe	Average
$T_m/6D$	0,048	0,049	0,048	0,048	0,048 ± 0,001
$1-(\rho_l/\rho_s)$	0,137	0,126	0,136	0,131	0,132 ± 0,005
$\Delta H_{mel}/D$	0,94	1,00	0,99	0,99	0,98 ± 0,03
$\varepsilon_{cv}/6D$	0,82	0,92	0,91	0,91	0,89 ± 0,04
ε_{vac}/D	8,3	8,6	8,0	8,3	8,3 ± 0,2
n_{vac}	45	37	59	45	46 ± 9

Weber[100] which was constructed on the basis of computer modeling of an argon cluster with the cubic body-centered lattice. It accounts for interaction of vacancies and the influence of excitations on the energy of the system. The interaction energies for both effects are assumed in this model to be proportional to the square of the number of single vacancies inside the system. This approximation gives the "S-bend" form for the temperature dependence of the cluster density. Such a form describes both the Stillinger and Weber phase transition in a macroscopic systems[100] and the phase coexistence. Because one can introduce strictly the interaction of vacancies for an atomic system with a short-range interaction, this allows us to check the validity of the above assumptions as long as the atom movement does not influence the state of the system.

Let us treat the Table I data on the basis of the above assumptions (see Table XI). The formation of vacancies inside a system demands a certain expenditure of energy. Assuming a decrease in the system density as a result of the phase transition to be connected with formation of vacancies, one can calculate by using the measured values of the specific energy of the process the energy which is expended per single vacancy ε_{vac}, i.e. the energy that is necessary to remove one atom from the system. Table XI contains the corresponding values of the specific energy for the formation of a single vacancy ε_{vac}.

The energy of formation of a single vacancy depends on its size. For example, it is necessary to break 12 bonds for the removal of one atom from inside of a system with a short-range interaction of atoms, i.e. $\varepsilon_{vac}=12D$. For removal of a diatomic molecule we must break 23 bonds, i.e. $\varepsilon_{vac} \sim 11.5D$. This accounts for an interaction of single vacancies which coalesce into bubbles. The energy for the formation of a single vacancy depends on bubble size. Using the energy per single vacancy which we obtain from measuring values of the heat of melting and the volume change on melting, one can evaluate the average vacancy size for melting of various condensed inert gases. Such an operation was made in Ref. 24 and the obtained values of a number of vacancies in a bubble n_{vac} are given in Table XI.

The above analysis is a logically consistent one within the framework of the used concept. Indeed, assuming that the liquid differs from the crystal consisting of atoms with a short-range interaction only by presence of vacancies inside it, we have estimated the average size of the vacancies by using experimental data. But it is difficult to explain the obtained result $n_{vac} \sim 50$ within the framework of the mathematical model. This casts doubt on the used mechanism of the phase transition and demands a search for alternative mechanisms for the phase transition.

The above result casts doubt also on the mechanism of the phase transition which is used by the Stillinger–Weber model.[100] According to this model the phase transition is created by vacancy interaction. This interaction for a macroscopic system of atoms with a short-range interaction can be found accurately on the basis of measuring the parameters of the phase transition and can explain the observed picture of the phase transition of condensed inert gases as a result of formation of bubbles consisting of dozens of vacancies inside a system. If we reject this conclusion, we must also regard the mechanism of the phase transition corresponding to the Stillinger–Weber model to be a doubtful one.

Using the analysis of the phase transition for surface layers of clusters with a short-range interaction of atoms, one can contend that its mechanism is explained by a nonlinear interaction of collective vibrations. Then symmetrical structures of clusters with a short-range interaction of atoms give one of such mechanisms of the phase transition. It will be considered below. Within the framework of this mechanism the phase transition inside condensed inert gases is determined by the interaction of the cubic face-centered and icosahedral structures.

There are three structures of clusters with close packing: cubic face-centered, hexagonal and icosahedral, and for each of these an internal atom of the structure has 12 nearest neighbors. Note that all inert gas crystals have the cubic face-centered lattice, and the phase transition to the hexagonal lattice is observed sometimes, but it demands special conditions and is accompanied by a small specific energy of transition. Therefore further we will not differentiate between the cubic face-centered and hexagonal structures, and consider the phase transition as a transition between the cubic face-centered and icosahedral structures.

The icosahedral structure is not advantageous at zero temperature because the distances between nearest neighbors of this structure differ from the optimal ones by approximately 2.5%. With increase of the temperature the amplitude of atom vibrations is increased and average distances between nearest atoms are increased also due to anharmonism of vibrations. Evidently, if this change approaches 2.5%, both the cubic face-centered and the icosahedral one can exist inside the crystal. This will correspond to a phase transition. As can be seen from Table XI, the solid-liquid phase transition for condensed rare gases corresponds to just such a change of the average distance between nearest atoms. Note that this concept of the phase transition does not mean the formation of clusters with the icosahedral structure inside the system. It shows only that the formation of intermediate cluster structures is useful for the description of this phenomenon.

Consider the solid-liquid phase transition inside a system with short-range interaction of atoms, as a result of formation of clusters with icosahedral structure inside it. It

means that an element of the crystal structure which is a cluster with the cubic face-centered structure is transformed into a cluster with the icosahedral structure as a result of displacement of its atoms. Then the cluster size is decreased and it can turn about its center. This is a mechanism of the atom displacement to new nodes of the crystal lattice without formation of vacancies inside the system.

Let us estimate the energy of the considered transition by assuming that it relates to a cluster consisting of 13 atoms (the minimum number of cluster atoms among the possible ones). As a result of the transition a cluster with the cubo-octahedral structure is transformed into a cluster with the icosahedral one. Assuming that the atoms surrounding this cluster retain their positions during the transition, we calculate the energy of such a transition. We take into account that both structures have one central atom and 12 atoms are located on a sphere. Because the transition from the cubo-octahedron to the icosahedron changes in an essential manner the atom distribution on the sphere, we assume that the atoms of the icosahedron are located on the sphere randomly with respect to the surrounding atoms of the lattice. Moreover, we use the expression (5b) for the pair potential of the short-range interaction of atoms:

$$U(R) = D \exp[-(R-R_e)^2/2\Delta r^2]. \tag{51}$$

We pick out inside an inert gas crystal a cubo-octahedron cluster consisting of 13 atoms. Its atoms have 84 bonds with surrounding atoms of the crystal. Therefore the removal of this cluster from the crystal demands an energy expenditure of $84D$. The above bonds involve 6 atoms which are located at a distance of $a\sqrt{2}$ from the cluster center, and each of these atoms has 4 bonds with cluster atoms. In addition, there are 24 atoms of the surrounding lattice at a distance of $a\sqrt{3}$ from the center and each of these has 2 bonds with cluster atoms, and 12 atoms with one bond are located at a distance of $2a$ from the center. Here a is the lattice constant and for the crystal with a short-range interaction of atoms we have $a=R_e$.

Let us determine the change in the potential of interaction of external atoms of the lattice with cluster atoms for the transition from a cubo-octahedron to an icosahedron. Assuming icosahedral atoms to be distributed on the sphere randomly, denote by R the sphere radius, R_1 the distance of an external atom from the cluster center and assume $R+R_e-R_1 \gg \Delta r$. Then the average interaction potential of an external atom with a cluster atom is equal to:

$$\bar{U} = \int_{-1}^{1} \frac{d\cos\alpha}{2} U[(R_1^2+R^2-2RR_1\cos\alpha)^{1/2}]$$
$$= \frac{R_e\Delta r}{RR_1} D \sqrt{\frac{\pi}{2}}, \tag{52}$$

where α is the angle between directions which join the atoms under discussion with the cluster center. From this it follows that the average interaction potential of cluster atoms with surrounding atoms of the lattice is equal to $\bar{U} = 272D\Delta r/R$ and this formula is the first term of expansion in terms of the small parameter $\Delta r/R_e$ under the assumptions made. Assuming near the minimum the pair

TABLE XII.

Shell	n_j	Number of bonds with cubo-octahedron	R_j/R_0
013	24	4	5
222	8	3	6
123	48	2	7
033	12	1	9

interaction potential to have the form of the Lennard–Jones one (4), we obtain for the binding energy of the icosahedral cluster with the face-centered lattice $\bar{U}=32D$.

Taking into account 36 bonds between nearest neighbors in the cubo-octahedron cluster of 13 atoms and 42 bonds in the icosahedron cluster of the same size, we will find the energy expenditure for the transition from a cubo-octahedron to an icosahedron inside the crystal lattice $\Delta\varepsilon = 47D$. We assume that at the melting point this energy is compensated by the vibration energy of atoms in the existing bonds, i.e. $nT_c = \Delta\varepsilon$, where T_c is the melting point. Then we obtain:

$$T_c = 0.56D. \tag{53}$$

This estimate corresponds to real values of the melting point for condensed inert gases $T_c = 0.58D$.

Let us make the same estimate for the cluster consisting of 55 atoms assuming that as a result of the cluster transition from a cubo-octahedron to an icosahedron the surrounding lattice retains the cubic face-centered structure. Table XII contains parameters of lattice atoms which interact with cluster atoms. Averaging over positions of the icosahedron atoms on the sphere, we obtain for the mean binding energy of the icosahedron with the surrounding lattice:

$$\bar{U} = D \sqrt{\frac{\pi}{2}} \Delta r \cdot R_0 \sum_{i,j} \frac{n_i}{R_i} \frac{n_j}{R_j}, \tag{54}$$

where n_i is the number of atoms in the corresponding icosahedral shell, R_i is the radius of this shell, n_j, R_j are the same parameters for atoms of the surrounding lattice which are given in Table XII.

For definiteness we assume the distances between atoms to be the same as in an isolated icosahedron cluster. Moreover, we used, as before, the short-range interaction potential in the form (5b) when the parameter Δr corresponds to the truncated Lennard–Jones interaction potential $\Delta r = R_e/\sqrt{72}$. Then atoms of the icosahedral surface include 12 atoms-vertices with $R_i = 1.936R_e$ and 30 atoms situated at the midpoints of sides of equilateral triangles with $R_i = 1.732R_e$. Moreover, the transformation of the cubo-octahedron cluster consisting of 55 atoms into the icosahedron cluster demands an energy expenditure of $13D$ under the above conditions.

Formula (54) gives in this case $\bar{U} = 112D$. This corresponds to the energy expenditure for the transformation of a cubo-octahedron cluster consisting of 55 atoms into an icosahedron cluster inside the crystal lattice $\Delta\varepsilon = 103D$. We assume that this energy expenditure is compensated at

the phase transition by the vibration energy nT_c on bonds between the cluster and the surrounding atoms. Because $n=228$, we obtain in this case

$$T_c = 0.45 D. \tag{55}$$

As can be seen, this estimate coincides within the limits of this accuracy with the preceding one and with the values of the melting point for inert gas crystals.

Thus the phase transition for a system of bound atoms with a short-range interaction can be explained as a result of nonlinear vibrations for modes which mix cubo-octahedral and icosahedral structures of clusters consisting of lattice atoms. Many atoms partake in such vibrations which can include both normal and tangential movements. These vibrations can be accompanied by a small rotation of clusters. A certain amplitude of these vibrations leads to formation of vacancies.

Vibrations which are responsible for the phase transition can be picked out in the course of the analysis of the motion spectrum for a system of bound atoms if this motion is modeled by computer methods of molecular dynamics. Amplitudes of motion for frequencies which correspond to vibrations which mix the cubo-octahedral and icosahedral structures must increase sharply near the temperature of the phase transition. Data on the parameters of these vibrations obtained from the numerical computer analysis of systems will allow us to construct a simple model of the phase transition which is similar to that of Ref. 100, but takes into account the real mechanism of the phase transition and its numerical parameters. The more accessible analysis of such a type relates to the phase transition of surface layers for clusters with filled shells, i.e. to the above symmetrical cluster structures.

Thus symmetrical structures of clusters assist progress in understanding the solid-liquid phase transition for atom systems with a short-range interaction of atoms. The mechanism of this transition is associated with a nonlinear interaction of collective vibrations of atoms in the system, that, probably, results from the transition between the cubo-octahedral and icosahedral structures of clusters inside the system.

10. CONCLUSION

The analysis of clusters with close packing shows that they are a convenient object for studies of systems of many bound atoms. Because of the high symmetry and simple description of such clusters, one can use these as a model for investigation of various problems of large clusters, especially, by using modern computer methods.[102,103] The symmetric cluster structures discussed above are useful in this regard due to their simplicity. The possibility examined above to analyze these structures within the framework of a general scheme allows one to obtain general conclusions about their structure, energy parameters and their role in various processes.

Clusters can form new stable structures (Refs. 104 and 105) which can be the basis of solids new in principle such as fullerenes.[106] Therefore, clusters can be used for assembling new materials (Refs. 49 and 107) and be a basis for

new technologies (Refs. 108–116). One of the stable cluster structures with close packing is a cluster with icosahedral structure which is realized in various solids. This structure is essential for various processes and interactions in systems with a short-range interaction of atoms, and the experience of this review confirms it.

The main problem of physics of large clusters relates to their correspondence with macroscopic particles. According to the accumulated experience in some cases we find such a correspondence, in other cases it is absent. For example, the surface energy of such a cluster is described by a macroscopic dependence $n^{2/3}$ with an accuracy of several percent starting from clusters with a few dozen of atoms. The reason for this is a large number of shells and atoms which give a contribution to the surface energy. Some properties of large clusters differ from macroscopic ones. For instance, the cluster cohesive energy is a nonmonotonic function of the number of cluster atoms up to thousands of atoms in a cluster in contrast to the properties of macroscopic particles. This is explained by the block structure of clusters with close packing, and each block includes hundreds of atoms. As a result, the cluster cohesive energy as a function of the number of atoms has an oscillating structure. These oscillations become nonessential for clusters consisting of $\sim 10^4$ atoms.

One would expect at the first stage of studies of large clusters that a cluster as a system intermediate between molecules and macroscopic particles has properties of one of these depending on its size.[117,118] It turned out, that a large cluster is an object with specific properties in a wide region of the number of atoms in it.[119–121] These properties depend on the cluster structure. Clusters with close packing as one kind of cluster give a useful experience in this direction. The simplicity of these clusters will allow them to be used as a model for studies of various processes and phenomena.

[1] C. Kittel, *Introduction to Solid State Physics*, 6th Ed., Wiley, N. Y., 1986.
[2] G. Leibfried, Gittertheory der Mechanischen und Termischen Eigenschaften der Kristalle. Handbuch VII, Teil 2, Springer Verlag, Berlin, 1965.
[3] C. Bunn, *Crystals*, Academic Press, N. Y., 1964.
[4] N. W. Ashcroft and N. D. Mermin, *Solid State Physics*. (Holt, Rinehart and Wilson, N. Y., 1976.
[5] A. L. Mackay, Acta Crystallogr. **15**, 916 (1962).
[6] S. Ino, J. Phys. Soc. Jpn **27**, 941 (1969).
[7] M. R. Hoare, Adv. Chem. Phys. **40**, 49 (1979).
[8] J. Farges, M. F. de Feraudy, B. Raoult, and G. Torchet, J. Chem. Phys. **78**, 5067 (1983).
[9] M. R. Hoare and M. McInnes, Adv. Phys. **32**, 791 (1983).
[10] J. Farges, M. F. de Feraudy, B. Raoult, and G. Torchet, Surf. Sci. **106**, 95 (1981).
[11] S. W. Wang, L. M. Falikov, and A. W. Searcy, Surf. Sci. **143**, 609 (1984).
[12] L. D. Marks, J. Cryst. Growth **61**, 556 (1984).
[13] L. D. Marks, Philos. Mag. **A49**, 81 (1985).
[14] A. Howie and L. D. Marks, Philos. Mag. **A49**, 25 (1985).
[15] J. A. Northby, J. Chem. Phys. **87**, 6166 (1987).
[16] J. W. Lee and G. D. Stein, J. Phys. Chem. **91**, 2450 (1987).
[17] H. G. Fritsche, Phys. Status Solidi **143**, K11 (1987).
[18] J. D. Honneycutt and H. C. Andersen, J. Phys. Chem. **91**, 4950 (1987).
[19] J. Farges, M. F. de Feraudy, B. Raoult, and G. Torchet, Adv. Chem. Phys. **70**, 45 (1988).

[20] B. Raoult, J. Farges, M. F. de Feraudy, and G. Torchet, Philos. Mag. **B60**, 881 (1989).

[21] B. W. van de Waal, J. Chem. Phys. **90**, 3407 (1989).

[22] J. A. Northby, J. Xie, D. L. Freemann, and J. P. Doll, Z. Phys. **D12**, 69 (1989).

[23] B. M. Smirnov, Sov. Phys. Usp. **35**, 37 (1992).

[24] B. M. Smirnov, Sov. Phys. Usp. **35**, 1052 (1992).

[25] Metal Clusters, (Eds.) F. Träger and G. zu Putlitz, Springer Verlag, Berlin, 1986.

[26] Microclusters, (Eds.) S. Sugano, Y. Nishina, and S. Ohnishi, Springer Verlag, Berlin, 1987.

[27] Physics and Chemistry of Small Clusters, (Eds.) P. Jena, B. K. Rao, and S. N. Khana, Plenum Press, N. Y., 1987.

[28] *Elemental and Molecular Clusters*, (Eds.) G. Benedek and M. Pachioni, Springer Verlag, Berlin, 1988.

[29] Atomic and Molecular Clusters, (Ed.) E. R. Bernstein, Elsevier, Amsterdam, 1990.

[30] B. M. Smirnov, *Cluster Ions and Van der Waals Molecules*, Gordon and Breach, Philadelphia, 1992.

[31] H. A. Bethe and P. Morrison, Elementary Nuclear Theory, Wiley, London, 1956.

[32] W. Pauli, Meson Theory of Nuclear Forces, IAS, Princeton, 1946.

[33] J. O. Hirschfelder, C. F. Curtiss, and R. B. Bird, *Molecular Theory of Gases and Liquids*, Wiley, N. Y., 1954.

[34] S. Chapman and T. G. Cowling, *Mathematical Theory of Non-Uniform Gases*, Cambridge University Press, Cambridge, 1952.

[35] J. H. Ferziger and H. G. Kaper, *Mathematical Theory of Transport Processes in Gases*, North Holland, Amsterdam, 1972.

[36] E. W. McDaniel and E. A. Mason, *Mobility and Diffusion of Ions in Gases*, Wiley, N. Y., 1973.

[37] K. P. Huber and G. Herzberg, *Molecular Spectra and Molecular Structure. IV. Constants of Diatomic Molecules*, Van Nostrand, N. Y., 1979.

[38] R. A. Azis. in *Inert Gas Potentials, Dynamics and Energy Transfer in Doped Crystals*, (Ed.) M. Klein, Springer Verlag, Berlin, 1984. P. 5.

[39] A. A. Radzig and B. M. Smirnov, *Reference Data on Atoms, Molecules and Ions*, Springer Verlag, Berlin, 1985.

[40] A. J. Moses, *Practicing Scientists Handbook*, Van Nostrand and Reinhold, N. Y., 1978.

[41] W. D. Knight, K. Clemerger, W. A. deHeer, W. A. Saunders, M. Y. Chou, and M. Cohen, Phys. Rev. Lett. **52**, 2141 (1984).

[42] H. Göhlich, T. Lange, T. Bergman and T. P. Martin, Phys. Rev. Lett. **65**, 748 (1990).

[43] S. Bjornholm, J. Borggreen, O. Echt, K. Hansen, J. Pedersen, and H. D. Rasmussen, Z. Phys. **D19**, 47 (1991).

[44] T. P. Martin, T. Bergmann, H. Göhlich, and T. Lange, Z. Phys. **D19**, 25 (1991)

[45] H. Göhlich, T. Lange, T. Bergman, U. Näher, and T. P. Martin, Chem. Phys. Lett. **187**, 67 (1992).

[46] D. A. Jelski, Z. C. Wu, and T. F. George, J. Cluster Sci. **1**, 147 (1990).

[47] C. L. Cleveland and U. Landman, J. Chem. Phys. **94**, 376 (1991).

[48] B. K. Teo and H. Zhang, J. Cluster Sci. **1**, 155 (1990).

[49] S. N. Khanna and P. Jena, Phys. Rev. Lett. **69**, 1664 (1992).

[50] B. Raoult and J. Farges, Rev. Sci. Instrum. **44**, 430 (1973).

[51] J. Farges, M. F. de Feraudy, B. Raoult, and G. Torchet, J. Chem. Phys. **78**, 5067 (1983).

[52] J. Farges, M. F. de Feraudy, B. Raoult, and G. Torchet, J. Chem. Phys. **84**, 3491 (1986).

[53] O. Echt, K. Satler, and E. Recknagel, Phys. Rev. Lett. **47**, 1121 (1981).

[54] O. Echt et al., Ber. Bunsenges, Phys. Chem. **86**, 860 (1982).

[55] A. Ding and J. Hesslish, Chem. Phys. Lett. **94**, 54 (1983).

[56] E. Recknagel et al., Ber. Bunsenges, Phys. Chem. **88**, 201 (1984).

[57] T. D. Märk and P. Scheier, Chem. Phys. Lett. **137**, 245 (1987).

[58] W. Miehle, O. Kandler, T. Leisner, and O. Echt, J. Chem. Phys. **91**, 5940 (1989).

[59] P. G. Lethbridge and A. J. Stace, J. Chem. Phys. **91**, 7685 (1989).

[60] T. P. Martin, T. Bergmann, H. Göhlich and T. Lange, Chem. Phys. Lett. **176**, 343 (1991).

[61] L. D. Landau and E. M. Lifshitz, *Statistical Physics*, Pergamon Press. N. Y., 1980.

[62] A. S. Kompaneets, *Theoretical Physics*, (In Russian), GITTL, M., 1957.

[63] A. I. Ansel'm, *Introduction to Semiconductor Physics* (In Russian), Fizmatgiz, M., 1962.

[64] P. C. Kireev. *Semiconductor Physics* (In Russian), Vysshaya Shkola, M., 1962.

[65] Ya. B. Zeldovich. Zh. Eksp. Teor. Fiz. **12**, 525 (1942).

[66] Ya. Frenkel, *Kinetic Theory of Liquids*, Oxford University Press, Oxford, 1946.

[67] W. S. Dunning, in *Nucleation*, (Ed.) A. C. Zettlemoyer, Marsell Dekker, N. Y., 1969, chap. 1.

[68] F. F. Abraham, *Homogeneous Nucleation Theory*, Academic Press, N. Y., 1974.

[69] J. J. Burton, in *Statistical Mechanics, A*, (Ed.) B. J. Berne, Plenum Press, N. Y., 1977, Ch. 6.

[70] E. M. Lifshitz and L. P. Pitaevskii, *Physical Kinetics*, Pergamon Press, Oxford, 1981.

[71] H. E. Stanley, *Introduction to Phase Transitions and Critical Phenomena*, Claredon Press, Oxford, 1971.

[72] J. W. M. Frenken and J. F. Van der Veen, Phys. Rev. Lett. **54**, 134 (1985).

[73] P. Buffat and J. P. Borel, Phys. Rev. **A13**, 2283 (1976).

[74] J. Bösiger and S. Leutwyler, Phys. Rev. Lett. **59**, 1985 (1987).

[75] M. Y. Hahn M. Y. and R. L. Whetten, Phys. Rev. Lett. **61**, 1190 (1988).

[76] T. Castro, R. Reifenberger, E. Choi, and R. P. Andres, Phys. Rev. **B42**, 8548 (1990).

[77] R. S. Berry, J. Jellinek, and G. Natanson, Phys. Rev. **30A**, 919 (1984).

[78] J. Jellinek, T. L. Beck and R. S. Berry, J. Chem. Phys. **84**, 2783 (1986).

[79] T. L. Beck, J. Jellinek and R. S. Berry, J. Chem. Phys. **87**, 545 (1987).

[80] H. Reiss, P. Mirabel and R. L. Whetten, J. Chem. Phys. **92**, 7241 (1988).

[81] U. Landman, in *Computer Simulation Studies in Condensed Matter Physics*, (Eds.) D. P. Landau, K. K. Mon, and H. B. Schuttler, Springer Verlag, Berlin, 1988.

[82] R. S. Berry, Phase Trans. **24–26**, 259 (1990).

[83] T. L. Beck and T. L. Marchioro, J. Chem. Phys. **93**, 1347 (1990).

[84] R. S. Berry, Sci. Am. **263**, 68 (May 1990).

[85] R. S. Berry, J. Chem. Soc. Faraday Trans. **86**, 2343 (1990).

[86] P. Ercolessi, W. Andreoni and T. Tosatti, Phys. Rev. Lett. **66**, 911 (1991).

[87] H. P. Cheng and R. S. Berry, Mat. Res. Soc. Symp. Proc. **206**, 241 (1991).

[88] H. P. Cheng and R. S. Berry, Phys. Rev. **45A**, 7969 (1992).

[89] H. P. Cheng, X. Li, R. L. Whetten, and R. S. Berry, Phys. Rev. **46A**, 791 (1992).

[90] Z. X. Cai, S. D. Mahanti, A. Antonelli, S. N. Khanna, and P. Jena, Phys. Rev. **B46**, 7841 (1992).

[91] W. N. Lipscomb, Science **153**, 373 (1966).

[92] R. B. King, Inorg. Chim. Acta, **49**, 237 (1981).

[93] B. F. G. Jonston, J. Chem. Soc. Chem. Commun. 27 (1986).

[94] D. J. Wales, J. Phys. Chem. **91**, 7002 (1989).

[95] D. J. Wales, Chem. Phys. Lett. **166**, 419 (1990).

[96] P. A. Braier, R. S. Berry, and D. J. Wales, J. Chem. Phys. **93**, 8745 (1990).

[97] D. J. Wales and R. S. Berry, J. Chem. Phys. **92**, 4283 (1990).

[98] H. D. Davis, D. J. Wales, and R. S. Berry, J. Chem. Phys. **92**, 4283 (1990).

[99] P. A. Braier and R. S. Berry, J. Chem. Phys. **93**, 8745 (1990).

[100] F. H. Stillinger and T. A. Weber, J. Chem. Phys. **81**, 5095 (1984).

[101] D. J. Wales and R. S. Berry, J. Chem. Phys. **92**, 4473 (1990).

[102] *Universalities in Condensed Matter*, (Ed.) R. Jullien, L. Peliti, R. Rammal, and N. Boccara, Springer Verlag, Berlin, 1988.

[103] *Computer Simulation Studies in Condensed Matter Physics*, (Ed.) D. P. Landau, K. K. Mon and H. B. Schuttler, Springer Verlag, Berlin, 1988.

[104] H. W. Kroto, J. R. Heath, S. C. O'Brien, R. E. Curl and R. E. Smalley, Nature **318**, 162 (1985).

[105] B. C. Guo, K. P. Kerns, and A. W. Castleman, Science **255**, 1411 (1992).

[106] W. Kräftschmer, L. D. Lamb, K. Fostiropolous, and D. R. Huffman, Nature **347**, 354 (1990).

[107] P. Jena, S. N. Khanna, B. K. Rao, and M. Manninen, Mat. Res. Soc. Symp. Proc. **206**, 3 (1991).

[108] T. Takagi, J. Vac. Science Technol. **A2**, 382 (1984).

[109] I. Yamada, H. Usui, and T. Takagi, J. Phys. Chem. **91**, 2463 (1987).

[110] T. Takagi, *Ionized-cluster Beam Deposition and Epitaxy*, Noyes Publication, N. J., 1988.

[111] J. Gspann, Z. Phys. **D20**, 421 (1991).

[112] O. F. Hagena, Z. Phys. **D20**, 425 (1991).
[113] J. Gspann, Z. Phys. **D20**, 421 (1991).
[114] O. F. Hagena, Rev. Sci. Instrum. **63**, 2374 (1992).
[115] J. Gspann, in *Physics and Chemistry of Finite Systems. From Clusters to Crystals*, (Eds.) P. Jena, B. K. Rao, and S. N. Khana, Kluwer Academic Publishers, Amsterdam, 1992.
[116] O. F. Hagena, G. Knop, and G. Linker, in *Physics and Chemistry of Finite Systems. From Clusters to Crystals*, (Eds.) P. Jena, B. K. Rao, and S. N. Khana, Kluwer Academic Publishers, Amsterdam, 1992.
[117] B. K. Rao, P. Jena, and D. D. Shillady, Phys. Rev. **B30**, 7293 (1984).
[118] B. K. Rao and P. Jena, J. Phys. **F16**, 461 (1986).
[119] J. L. Martins, J. Buttet, and R. Car, Phys. Rev. **B31**, 1804 (1986).
[120] B. K. Rao and P. Jena, Phys. Rev. **B32**, 2058 (1986).
[121] B. K. Rao, S. N. Khanna, and P. Jena, Phase Transitions **24–26**, 35 (1992).
[122] A. R. Ubbelohde, *The Molten State of Matter*, Wiley, Chicester, 1978.

The English text of this article was supplied by the author. It differs in many places from the Russian text in Usp. Fiz. Nauk, and should therefore be regarded as a translation combined with a revision. (*Translation Editor*)